



Microbial Mediated Synthesis of Zinc Oxide Nanoparticles, Characterization and Multifaceted Applications

Eman Zakaria Gomaa¹

Received: 27 April 2022 / Accepted: 1 June 2022 / Published online: 7 July 2022
© The Author(s) 2022

Abstract

Nanoparticles have gained considerable importance compared to bulk counterparts due to their unique properties. Due to their high surface to volume ratio and high reactivity, metallic and metal-oxide nanostructures have shown great potential applications. Among them, zinc oxide nanoparticles (ZnONPs) have gained tremendous attention attributed to their unique properties such as low toxicity, biocompatibility, simplicity, easy fabrication, and environmental friendly. Remarkably, ZnONPs exhibit optical, physical, antimicrobial, anticancer, anti-inflammatory and wound healing properties. These nanoparticles have been applied in various fields such as in biomedicine, biosensors, electronics, food, cosmetic industries, textile, agriculture and environment. The synthesis of ZnONPs can be performed by chemical, physical and biological methods. Although the chemical and physical methods suffer from some disadvantages such as the involvement of high temperature and pressure conditions, high cost and not environmentally friendly, the green synthesis of ZnONPs offers a promising substitute to these conventional methods. On that account, the microbial mediated synthesis of ZnONPs is clean, eco-friendly, nontoxic and biocompatible method. This paper reviews the microbial synthesis of ZnONPs, parameters used for the optimization process and their physicochemical properties. The potential applications of ZnONPs in biomedical, agricultural and environmental fields as well as their toxic aspects on human beings and animals have been reviewed.

Keywords Zinc oxide nanoparticles · Biosynthesis · Mechanism · Characterization · Biomedical applications · Nanofertilizer · Photocatalyst · Toxicity

1 Introduction

Nanotechnology has become the center of research interest for its potential to manufacture the materials on the scale of nano-size (up to 100 nm) [1]. Due to their extremely small size and high surface area to volume ratio, nanoparticles (NPs) exhibit unique optical, mechanical, catalytic, and biological properties over their bulk counterparts [2].

Metal oxide nanoparticles have received considerable research attention due to their pronounced properties and their wide range of applications [3]. Among them, zinc oxide nanoparticles (ZnONPs) have been extensively investigated because of their valuable properties such as biocompatibility, eco-friendly, low cost and ease of fabrication, high photosensitivity, large excitation binding energy, high thermal

conductivity, and stability under harsh environmental conditions [4]. Due to the numerous valuable properties of ZnONPs, these NPs are widely used in several fields such as in electronics, optics, food packaging, cosmetic products, petroleum industries, pharmaceuticals, and agriculture. Next to these applications, ZnONPs are widely used in biomedical applications including anticancer, antimicrobial, antioxidant, anti-inflammatory, wound healing and drug delivery [5]. In addition, ZnONPs have well-known as an effective photocatalyst agent that offers a promising method for wasted water treatment [6].

There are various methods that have been used for the preparation of ZnONPs such as physical, chemical and biological methods [7]. The physical and chemical methods suffer from a lot of disadvantages such as high cost, requirement of high throughput equipments and production of toxic by-products that could be harmful to the body or the ecosystem [8]. The green synthesis method is cleaner, economical, environmentally safe, and biocompatible alternatives that overcome all these limitations [9]. In particular,

✉ Eman Zakaria Gomaa
emann7778@yahoo.com

¹ Department of Biological and Geological Sciences, Faculty of Education, Ain Shams University, Cairo, Egypt

microorganisms have various biomolecules involved in ZnONPs synthesis either intracellularly or extracellularly [10]. Microbial synthesis of NPs provides large scale production of well-defined size and morphology [11].

This review emphasizes the microbial mediated synthesis of ZnONPs, the mechanisms of their synthesis and factors affecting the process. It also demonstrates various biomedical applications of ZnONPs owing to their antibacterial, antifungal, anticancer, anti-inflammatory and wound healing activities. The mechanisms of interaction of ZnONPs against a variety of microbes and factors affecting their antimicrobial properties have also been discussed in details. Furthermore, the potential applications of ZnONPs in the agricultural and environmental fields have been investigated.

2 Microbial Mediated Synthesis of ZnONPs

ZnONPs can be synthesized using chemical, physical, and biological methods. Chemical methods include microemulsion, reduction, sol–gel hydrothermal, and precipitation. Physical techniques can be performed by spray pyrolysis, vapor deposition, plasma and ultrasonic irradiation [12]. Nonetheless, these techniques usually involve the use of toxic chemicals, high temperature and pressure, costly equipments and machines [13]. Thus, there is a high need to apply a cost-effective and environment-friendly method for the synthesis of NPs.

The biological method is a promising alternative for the synthesis of NPs. This method is superior to other methods because it is safe, simple, non-toxic, eco-friendly, biocompatible, and cost-effective. In this process, ZnONPs is performed using biologically active materials produced by microorganisms or extracted from plant parts [14]. These biologically active products act as reducing and capping agents for NPs synthesis. In general, the biosynthesis of ZnONPs is a very straightforward process, in which metal precursor, in the form of soluble salts, was introduced to the previously prepared biological extracts. After the reaction time, a visible change in color occurred and ZnONPs powder is obtained [15]. Nonetheless, the green synthesis of NPs can also enhance the properties of the produced NPs due to the specific properties of the biological substrates used and the small size and shape obtained [16]. For instance, the green synthesis route of ZnONPs has been shown to improve the properties like antimicrobial activity, biocompatibility, and photocatalytic efficacy [17].

The NPs synthesis using microorganisms such as bacteria, fungi offers an advantage over plants since microbes are easily reproduced. The microbial synthesis of metal and metal oxide NPs depends on the tolerance of microbes to heavy metals. Generally, microbes that inhabit ecological niches rich in metal exhibit high metal resistance due to

adsorption of metals and their chelation by intra- and extracellular proteins [18]. The existence of various enzymes, biomolecules and proteins in microorganisms are recognized as capping agents in the formation of multiple sized NPs [19]. As such, this demonstrates their capability to act as natural nano-factory. Table 1 summarizes several microbes that mediate the synthesis of ZnONPs including their sizes and shapes.

2.1 Bacteria-Mediated Synthesis of ZnONPs

Bacteria were among the first organisms used for the production of NPs due to their feasibility of isolation, fast manipulation and the presence of natural mechanisms for metal ions detoxification [20]. There are many examples reported in the literature that generated ZnONPs using bacterial strains. For example, Selvarajan and Mohanasrinivasan [21] investigated the intracellular synthesis of pure crystalline and spherical shaped ZnONPs with the size ranged from 7 to 19 nm from *Lactobacillus plantarum* VITES07. It was reported that produced NPs were moderately stable, which indicated that the biomolecules secreted by the bacterial strain acted as a capping agent in the synthesis process. In addition, spherical shaped ZnONPs with the size range of 100–130 nm had been synthesized using *Rhodococcus pyridinivorans* and zinc sulphate as a substrate. The synthesis of these NPs was confirmed through the field emission scanning electron microscope (FESEM) and XRD analysis [22].

Saravanan et al. [5] used *Bacillus megaterium* cell free extract as unique reducing and capping agent for the synthesis of ZnONPs. The UV spectrum of the ZnONPs displayed the surface plasmon resonance (SPR) peak at 346 nm, while FESEM analysis showed that the produced ZnONPs were rod and cubic shaped with a diameter ranged from 45 to 95 nm. Similarly, Abinaya et al. [23] demonstrated a novel and effective approach to synthesize ZnONPs using the exopolysaccharides (EPS) from the probiotic strain *Bacillus licheniformis* Dahb1. The EPS acted as a reducing and stabilizing agent for the formation of NPs. The produced NPs were crystalline structure with a hexagonal shape and a size range between 10 and 100 nm.

2.2 Fungi-Mediated Synthesis of ZnONPs

Fungi are extremely versatile living organisms which have been also investigated for the production of ZnONPs. In comparison to the bacterial synthesis, it is believed that fungi may have superior potential for the green synthesis of NPs. Fungi have great tolerance to high metal concentrations due to their metal binding and bioaccumulation capacities [24]. Moreover, the fungi exhibited the ability to secrete a large number of extracellular redox proteins and enzymes, which contributed to the reduction of the metal ions into

Table 1 Microbes mediated synthesis of zinc oxide nanoparticles

Microbes	Size (nm)	Shape	References
<i>Acinetobacter schindleri</i>	20–100	Spheres	[185]
<i>Aeromonas hydrophila</i>	57.72	Spherical, oval	[71]
<i>Bacillus megaterium</i>	45–95	Rod and cubic	[5]
<i>Bacillus licheniformis</i>	200	Nanoflower	[22]
<i>Halomonas elongate</i>	18.11	Multiform	[186]
<i>Lactobacillus johnsonii</i>	4–9	Spherical	[31]
<i>Lactobacillus plantarum</i>	7–19	Spherical	[21]
<i>Lactobacillus sporogens</i>	5–15	Hexagonal	[187]
<i>Pseudomonas aeruginosa</i>	35–80	Spherical	[188]
<i>Rhodococcus pyridinivorans</i>	100–120	Roughly spherical	[189]
<i>Serratia ureilytica</i>	170–250	Spherical, nanoflower	[19]
<i>Sphingobacterium thalpophilum</i>	40	Triangle	[190]
<i>Staphylococcus aureus</i>	10–50	Circular	[29]
<i>Streptomyces sp.</i>	20–50	Spherical	[191]
<i>Candida albicans</i>	25	Quasi-spherical	[192]
<i>Pichia kudriavzevii</i>	10–61	Hexagonal	[43]
<i>Alternaria alternata</i>	45–150	Spherical, triangular, hexagonal	[193]
<i>Aspergillus aeneus</i>	100–140	Spherical	[31]
<i>Aspergillus fumigatus</i>	60–80	Spherical	[194]
<i>Aspergillus niger</i>	61	Spherical	[37]
<i>Aspergillus terreus</i>	54.8–82.6	Spherical	[195]
<i>Fusarium spp.</i>	> 100	Triangle	[196]

NPs [25]. The secreted proteins conferred the stability of the produced NPs by acting as capping agents that bound and encapsulated the NPs surface [26]. In this respect, *Aspergillus* species have been widely employed for the synthesis of ZnONPs. For instance, ZnONPs with the average size of 3.8 nm were synthesized from the mycelia of *Aspergillus fumigatus*. The produced NPs were stable without any agglomeration for 90 days [27]. Similarly, the biomass extracted from *Aspergillus niger* was used for the synthesis of ZnONPs following a co-precipitation method [28].

3 Mechanisms of Microbial Mediated Synthesis of ZnONPs

The determination of the microbial synthesis mechanisms of ZnONPs is of great interest for establishing large scale process. There are several studies propose the theoretical mechanistic routes for this biosynthesis. Thus, in this review, some of these studies found in the literature related to the mechanisms of ZnONPs formation have been reviewed.

The biosynthesis of metal and metal oxide NPs using microorganisms may occur in extra or intracellular environments [29]. In the case of the extracellular synthesis, studies suggested that the enzymes and proteins produced and released by the microorganisms can reduce the metal ions and stabilize the particles. In this respect, Tripathi et al. [22]

reported that ZnONPs can be stabilized by enzymes secreted by *Bacillus licheniformis*. The enzymes avoid agglomeration and increasing the nanoscale size of the metal oxide. Hulkoti and Taranath [30] reported that the bioreduction of Zn^{2+} was initiated by the electron transfer from NADH by NADH-dependent reductase that acts as an electron carrier. Consequently, the Zn^{2+} obtained an electron and reduced to ZnO. Subsequently, this resulted in the formation of ZnONPs. Other studies have shown that the proteins produced and secreted by microbes played an important role in the NPs synthesis. In this line, Jain et al. [31] revealed that the amino acids present in the protein were found to interact with the Zn^{2+} ions to form ZnONPs. Likewise, the production of metal and metal oxide NPs using fungal biomass or culture has a similar mechanistic route as the described for bacteria. Kalpana et al. [32] successfully synthesized ZnONPs using *Aspergillus niger* cell-free filtrate. They suggested that the proteins and enzymes secreted by this microorganism are responsible for the formation and encapsulation of the nanomaterials.

Regarding the intracellular synthesis, the mechanism of formation definition can be more challenging due to the complexity of the cell compositions and processes. However, various studies believed that the cells internalize the metallic ions which will be reduced by the proteins and enzymes within the cell to form the NPs [30]. The cell wall of microbes consists of a variety of polysaccharides

and protein, which provides active sites for the binding of the metal ions. This is due to the fact that metal ions are attracted to the negative charge of the carboxylate groups that is present on the cell wall. Then, the trapped ions are reduced into the elemental atom initiated by the electron transfer from NADH by NADH-dependent reductase that acts as an electron carrier, which is embedded in the plasma membrane. The reduction of the metal ion within the cell wall leading to the aggregation of metal atoms and formation of metal NPs [33]. In addition, the protein or peptides and amino acids such as cysteine, tyrosine and tryptophan exist in the cells are responsible for providing stabilization of NPs [34]. The authors reported the presence of metal NPs on the cytoplasmic membrane by transmission electron microscopy (TEM) analysis, which suggested that the formation of NPs occur in the cell wall and the cytoplasm of the cell [13]. However, it was indicated that the extracellular formation is the most common route to produce ZnONPs. The intracellular route requires an additional process of cell lysis to release the NPs from inside the microorganism. Hence, this process becomes more time consuming and expensive than the extracellular synthesis in which the metal ions are directly reduced by the proteins and enzymes outside the cells [35].

4 Factors Affecting the Microbial Mediated Synthesis of ZnONPs

It is well understood that the physicochemical properties of NPs are highly dependent on their size and morphology structures. Therefore, in order to generate high yield production of NPs with effective morphologies and size distribution, it is necessary to optimize the cultural conditions and physical parameters. Some of the parameters which are important to determine the rate of production, yield, morphologies and the physical–chemical properties of the ZnONPs are reviewed.

4.1 Effect of pH

Generally, pH is a key factor that has a major role in the synthesis of NPs and could modify their properties. pH has the ability to alter the shape of biomolecules that is responsible for the capping and stabilizing of NPs [36]. In this respect, Nagarajan and Kuppusamy [37] have investigated the variation of pH on ZnONPs synthesis. They reported that the increase of the pH values led to a decrease on particle size and agglomeration. At low pH range (pH 5–7), accumulation of ZnONPs occur to form larger particles, whereas at high pH value (pH 8) this accumulation does not occur. However, Singh et al. [9] states that a neutral pH would be the best condition for the biosynthesis of ZnONPs. This conclusion was based on the fact that the formation of $\text{Zn}(\text{OH})_2$ might

take place in alkaline pH solutions, which can alter the production of ZnONPs.

4.2 Effect of Temperature

The impacts of various temperatures on the size and yield production of NPs have been extensively investigated. For instance, Singh et al. [9] studied the influence of the temperature variation (20–100 °C) on the yield and size of ZnONPs. They concluded that the higher the temperature, the greater the yield of ZnONPs. However, increasing the temperature of reaction mixture resulted in the formation of NPs with a larger size. In addition, Bala et al. [38] indicated that changing of the temperature of the reaction mixture resulted in different morphologies and sizes of the ZnONPs. Irregular morphology and low crystallinity of the produced NPs were observed at 30 °C. In contrast, the NPs obtained at 60 °C and 100 °C presented high crystallinity and agglomerates of NPs. These variations are probably related to the fact that higher temperatures increase the nucleation rate of crystal formation. Another feature related to the agglomeration is that the interval of time of the heat treatment may affect the formation of clusters. Dhadapani et al. [39] observed that increasing the time of the thermal treatment conducted at 50 °C from 30 to 90 min, increased agglomerates and NPs growth.

4.3 Effect of Precursor Concentration

The impact of various precursor salt concentrations on the synthesis of metal NPs using soil fungus *Cladosporium oxysporum* was studied by Bhargava et al. [40]. They revealed that the precursor salt concentration of 1.0×10^{-3} mol/l gave a maximum NPs yield. At the concentrations of 2.0×10^{-3} and 5.0×10^{-3} mol/l, no NPs were generated due to the insufficient of biomolecules in minimizing the high amount of metal ions present. This finding is in agreement with Chinnasamy et al. [41] who concluded that the concentration of zinc nitrate is the factor that influences mostly the particle size among all the evaluated parameters. They stated that by using the minimum concentration of zinc precursor (~65 g/l) resulted in the highest yield of ZnONPs. On the other hand, Jamdagni et al. [42] observed that the absorbance of ZnONPs increased with the increasing of precursor concentration.

4.4 Effects of Microbial Age and Reaction Time

The growth phase of the microbial cell has a critical role for the synthesis of NPs. Since microbes generate various enzymes at different growth phases, controlling the cell age may be useful in producing high yields of NPs. It is well known that the cell at the early exponential stage actively

generated high concentrations of enzymes and protein, which resulted in a high reduction of metals and formation of NPs. Concerning the effect the reaction time, it was reported that rapid synthesis of NPs resulted in the formation of smaller size NPs. In this line, it was reported that in the synthesis of ZnONPs by *Pichia kudriavzevii* at a reaction time of 12 and 24 h, the small sized of NPs were generated. Whereas, prolonged reaction time to 36 h produced aggregate with irregular-shaped NPs [43]. In contrast, the synthesis of ZnONPs by *Lactobacillus* sp. yielded NPs with an average size of 7 nm at 5 to 10 min of reaction time [21]. Also, Chinnasamy et al. [41] reported that at a time reaction of 2 h, the highest yield of ZnONP was recorded.

Overall, the optimization process is essentially required to produce the desired NPs size, shape, yield, and homogeneous particles (monodispersity), mainly because these NPs have a significant role in determining their unique properties for specific applications. The study is still ongoing because each microbe has a wide range of abilities in producing NPs and further investigation is required to improve the synthesis process for implementation in practice.

5 Characterization of ZnONPs

The NPs are characterized physicochemically to determine their properties including size, shape, surface charge, functional groups, and the purity. Several techniques can be used to determine these properties such as ultraviolet- (UV-) visible spectroscopy, scanning electron microscopy (SEM), Transmission Electron Microscopy (TEM), Dynamic light scattering (DLS), Fourier transform infrared spectroscopy (FTIR), X-ray diffraction (XRD), Energy Dispersive X-ray Spectroscopy (EDS), and Thermo-gravimetric analysis (TGA) [44]. These commonly structural and chemical characterization used techniques are as follows:

5.1 UV-Visible Spectroscopy

UV-visible spectroscopy refers to absorption spectroscopy on reflectance spectroscopy in the ultraviolet-visible spectral region. Molecules containing non-bonding electrons or π electrons absorb energy in the form of UV or visible light to excite these electrons to higher anti-bonding molecular orbital. The more easily excited the electrons the longer the wavelength of light it can absorb. This technique is used to measure the maximum absorbance of the particle in certain wavelength. UV-visible spectra can be used to examine the size and shape-controlled NPs in aqueous suspension. In UV-visible spectroscopy, the decrease in intensity of original extinction peak gives information about particles destabilization and peak broadening or secondary peak occur at longer wavelength can be resulted from the increase in the

metal concentration beyond a threshold value or the formation of aggregates. Thus, the stability and the extent of NPs aggregation can be determined [45].

The optical property of ZnONPs is determined via UV-visible spectroscopy in the range of 200 nm–800 nm. The decrease in the particle size influences the intensity of absorption peak and shifts towards lower wavelength (blue shift). ZnONPs usually show an absorption peak in the range of 360–380 nm, a characteristic band for pure ZnO which indicates excitation of valence electrons of ZnONPs absorbing light in the UV region [46].

5.2 Scanning Electron Microscope (SEM)

SEM is used for the determination of surface morphology, homogeneity, and size of the NPs. It has the advantage of its versatile applications such as ease of sample preparation, different modes of imaging and easy interpretation of the images [47]. The Scanning electron microscope (SEM) uses a focused beam of high-energy electrons to generate a variety of signals at the surface of solid specimens. The signals that derive from electron sample interactions reveal information about the sample including external morphology, chemical composition, orientation of materials making up the sample, and their crystalline structure. The samples were made more viable when coated with gold sputtering. In addition, SEM images are useful in obtaining surface topological information of different NPs because of higher magnification and larger field depth, which depend on the electron density of the surface. The size, surface morphology, and aggregation of ZnONPs can be examined using the SEM images [48].

5.3 Transmission Electron Microscopy (TEM)

TEM uses energetic electrons to determine morphological, compositional, and crystallographic properties of the sample. The optimum resolution obtained from TEM images is much better than that for the light microscope as the wavelength of electrons is smaller than that of the light. Therefore, the fine details of internal structure can be resolved [49]. High-resolution TEM (HR-TEM) is a promising tool to study the properties of materials on the atomic scale, such as nanoparticles. The morphological characteristics and the size of the fabricated ZnONPs were studied with the help of TEM, featuring an ultra high resolution and rapid data acquisition [50].

5.4 Dynamic Light Scattering (DLS)

DLS is routinely used for NPs size determination, size distribution and zeta potential in solution. DLS measures time-dependent fluctuations of light scattered by NPs in

suspension undergoing Brownian motion and relates its velocity to the size of NPs, according to the Stokes-Einstein equation [51]. DLS provide information about the average size, size distribution by measuring the timescale of light intensity fluctuations. The resolving power in constant instrument settings depends on the ratio of size and mass of the species in a mixture, the dispersion characteristics and the total concentration of material [12].

5.5 Fourier Transform Infrared Spectroscopy (FTIR)

FTIR is an essential technique for the identification of the functional groups involved in the reduction and stabilisation of NPs. In FTIR spectroscopy, the sample is exposed to IR radiations and it selectively absorbs radiation of a specific wavelength which causes a change in the dipole moment and leads to transfer of vibrational energy level from the ground to the excited state. Vibrational energy gap determines the frequency of absorption peak.

The FTIR spectra are collected after the absorption of electromagnetic waves with the frequency range from 400 to 4000 cm^{-1} . The FTIR spectrometer gathers the spectral information of a broad spectral region. Metal oxide shows absorption bands in the fingerprint region below 1000 cm^{-1} attributed to interatomic vibration. ZnO shows vibrational peaks in the region between 400 and 600 cm^{-1} [52]. All the present peaks are attributed to the phytochemical components present in the synthesis of ZnONPs. The differences in the particle size may lead to different wave number and frequencies.

5.6 X-ray Diffraction Technique (XRD)

XRD is a powerful technique which gives information about the structure, average size and crystalline nature of a sample. Different lattice planes cause simultaneous reflections of the X-ray beam incident on a crystal. This may lead to constructive or destructive interference depending on the angle of incidence of X-rays and wavelength of X-rays. Crystalline solid has its unique characteristic X-ray diffraction pattern which is referred to as a “fingerprint” for its identification. Sharp and narrow diffraction peaks imply high crystallinity and small size of the biosynthesized NPs [53]. In the study of Kumar et al. [54], X-ray diffraction of the prepared ZnONPs used X-ray beam with nickel filtered $\text{CuK}\alpha$ radiations of wavelength equal to 1.54 Å and with a step dimension of 0.01° and scanning speed of 0.02 steps / second. A fixed power generation of 40 kV and 40 mA was used. The XRD pattern showed major peaks of diffraction angles are 31.61°, 34.23°, 36.35°, 47.63°, 56.32°, 62.79°, 66.97°, 67.02°, 69.37°, and 76.18° which correlating to reflection planes are 100, 002, 101, 102, 110, 103, 200, 112, 201, and 202 respectively.

5.7 Energy Dispersive X-Ray Spectroscopy (EDS)

EDS is used to determine the chemical characterization and elemental composition of NPs and it is usually integrated with either scanning electron microscope (SEM) or electron probe microanalyzer (EPMA). EDS consist of an X-ray detector, liquid nitrogen for cooling, and software to collect energy spectra. A crystal in the EDS detector absorbs the energy of incoming X-rays by ionization, induces free electrons in the crystal that are conductive and creates a bias in electrical charge. The energy of individual X-rays converts into electrical voltages of proportional size by X-ray absorption. The electrical pulses correlate to the characteristic X-rays of the elements, which can be used for elemental identification [55].

5.8 Thermo-gravimetric Analysis (TGA)

The thermal analysis of NPs determines the properties like enthalpy, mass changes, thermal capacity and the coefficient of heat expansion. TGA is a technique used to determine the change in mass of a sample as a function of temperature and/or time in a controlled atmosphere and rapid assessment of the thermal stability of substances. Change in the mass of a sample can occur from thermal decomposition, evaporation, drying, sublimation, desorption or adsorption. These changes in mass are shown as step changes in the TGA curve or peaks in the DTG curve. The properties of nanomaterials are determined according to how they change with temperature by thermal analysis and the results such as descending TGA thermal curve indicates the weight loss that has occurred [56].

6 Application of ZnONPs

6.1 Biomedical Applications of ZnONPs

ZnONPs, as a type of the low-cost and low-toxicity nanomaterials, have attracted tremendous interest in various biomedical fields due to their antimicrobial, anticancer, anti-inflammatory, and wound healing activities [57]. Some of these activities which support their biomedical applications are reviewed.

6.1.1 Antimicrobial Activity of ZnONPs

Microbial diseases pose serious health threats among mankind. The spreading of multidrug-resistant microbes and emergence of new strains makes the need for developing new effective techniques become urgent. Nanotechnology has emerged as a novel approach to fight microbial diseases and can be used for the effective treatment of pathogenic

microbial diseases [58]. The antimicrobial properties of nanomaterials arise from their inherent properties, such as high reactivity due to large surface area to volume ratio, composition and morphology that allow the nanomaterials to interact easily with the microbial cell surface and subsequently exhibit their antimicrobial mechanisms [59].

The antimicrobial effect of ZnONPs is remarkable due to their unique physiochemical properties such as smaller size, higher porosity and larger specific area. In addition, ZnONPs are also found to be safe and compatible with the human system [60]. Some studies concerning the antibacterial and antifungal activities of ZnONPs have been reviewed. ZnONPs showed potent antibacterial activity towards both gram-positive and gram-negative bacteria such as, *Bacillus subtilis*, *Salmonella typhimurium*, *Staphylococcus aureus*, *Streptococcus pyogenes*, *Enterococcus faecalis*, *Proteus mirabilis*, *Escherichia coli*, *Klebsiella pneumoniae*, *Klebsiella aerogenes*, *Mycobacterium tuberculosis*, *Mycobacterium luteus*, *Proteus vulgaris*, *Vibrio cholera*, *Pseudomonas aeruginosa*, *Salmonella typhimurium* and *Salmonella paratyphi* [61–63]. The antibacterial effects of ZnONPs in different bacterial species are cited in Table 2. The minimum inhibitory concentration (MIC) of ZnONPs for *Staphylococcus aureus* and *Escherichia coli* were reported as 12.5 and 6.25 µg/ml, respectively [64]. Wherese, Shamshad et al. [65] found that MIC of ZnONPs was 100, 11.1 and 3.7 µg/ml

for *Staphylococcus aureus*, *Pseudomonas aeruginosa* and *E. coli*, respectively.

Dulta et al. [66] reported that the green synthesized ZnONPs showed antimicrobial effects against Gram negative microorganisms with lowest MIC value recorded as 6.25 µg/ml. Furthermore, the antibacterial effect showed the slightly superior of the ZnONPs prepared by chemical method on the prepared by green method at levels 50 and 100 ppm, while no differences found at 150 ppm in *Pseudomonas aeruginosa* and *B. subtilis*. On the other hand, the comparable results for two ZnONPs in *S. aureus* [67]. In addition, Raghavendra et al. [68] reported that among all the tested bacterial pathogens, *E. coli* at 50 µg/ml concentration showed the highest inhibition of biofilm activity upon treatment with the biosynthesized ZnONPs, followed by the highest growth curve, cellular leakage, and potassium ion efflux.

Moreover, ZnONPs were demonstrated as an anti-biofilm and anti-virulence compound. In this trend, the antibiofilm activity of the biosynthesized ZnONPs were studied by Jayabalan et al. [69] against *Pseudomonas otitidis* (MCC2509), *Pseudomonas oleovorans* (MCC2566), *Acinetobacter baumannii* (MCC2366), *Bacillus cereus* (MCC2039), and *Enterococcus faecalis* (MCC2041). The results revealed that ZnONPs showed very potent activity against the tested microbial biofilms. Also, Abdelraheem and Mohamed [70]

Table 2 The antibacterial effects of ZnONPs in different bacterial species

Material	Size (nm)	Targeted bacteria	Antibacterial mechanism	Reference
ZnONPs	30	<i>E. coli</i>	Destroy the membrane integrity and ROS production	[197]
ZnONPs	20	<i>E. coli</i> 11,634	Hydrogen peroxide (H ₂ O ₂)	[198]
ZnONPs	20	<i>E. coli</i> and <i>S. aureus</i>	Release of Zn ²⁺	[199]
ZnONPs	40	<i>Streptococcus mutans</i> (MTCC497), <i>S. pyogenes</i> (MTCC1926), <i>Vibrio cholerae</i> (MTCC3906), <i>Shigella flexneri</i> (MTCC1457), and <i>Salmonella typhi</i> (MTCC1252)	ROS and the release of Zn ²⁺	[83]
ZnONPs	80	<i>V. cholera</i>	Depolarization of the membrane structure, increased permeabilization and damage of DNA, and generation of ROS	[200]
ZnONPs	90–100	<i>V. cholera</i> and enterotoxigenic <i>E. coli</i> (ETEC)	Inhibit adenyl cyclase activity, and cAMP levels are decreased	[201]
Ag-ZnO composite	64	<i>S. aureus</i> and GFP <i>E. coli</i>	ROS and the release of Ag ⁺ and Zn ²⁺	[202]
ZnO nanocatalyst	18	<i>B. subtilis</i> , <i>E. coli</i> , <i>K. pneumoniae</i> , and <i>S. typhimurium</i>	H ₂ O ₂ , OH ⁻ , and other ROS	[203]
ZnO quantum dots	4	<i>E. coli</i> MG1655, <i>Cupriavidus metallidurans</i> CH ₃₄	the toxicity is mainly from Zn ²⁺	[204]
CdO-ZnO nanocomposite	27	<i>E. coli</i> , <i>P. aeruginosa</i> , <i>Klebsiella pneumoniae</i> , <i>S. aureus</i> , <i>P. vulgaris</i> , and <i>Bacillus</i> spp	ROS (OH ⁻ , H ₂ O ₂ , and O ₂ ²⁻) and the release of Zn ²⁺ and Cd ²⁺	[205]
ZnO nanostructures (ZnO-NSs)	70–80	<i>S. aureus</i> , <i>S. typhimurium</i> , <i>P. vulgaris</i> , and <i>K. pneumoniae</i>	ROS damage to cell membranes	[206]

confirmed that ZnONPs significantly down-regulated the expression level of all biofilms and virulence genes of *P. aeruginosa* clinical isolates except the *toxA* gene.

In addition to their antibacterial activity, ZnONPs have also been reported to perform a promising antifungal activity against many of the harmful yeasts and fungi. In this respect, Jayaseelan et al. [71] reported that ZnONPs synthesized using *Aeromonas hydrophila* exhibited pronounced antifungal activity against various fungal pathogens such as *Aspergillus flavus*, *Aspergillus niger* and *Candida albicans*. Also, Rajiv et al. [72] validated the antifungal activity of ZnONPs and found that the activity is size-dependent and the highest inhibition was reported against *Aspergillus flavus* and *Aspergillus niger* at 25 µg/ml. Furthermore, Jamdagni et al. [42] showed an antifungal activity of ZnONPs against five of the fungal pathogens of plants such as *Alternaria alternata*, *Aspergillus niger*, *Botrytis cinerea*, *Fusarium oxysporum* and *Penicillium expansum* and the lowest minimum inhibitory concentration of 16 µg/ml was reported against *A. niger*. In addition, Vijayakumar et al. [73] proved the antifungal activity of ZnONPs at a concentration of 100 µg/ml, against *Candida albicans*, a most prevalent fungal pathogen. Moreover, Jain et al. [74] indicated that the synthesized ZnONPs using *Serratia nematodiphila* showed good antimicrobial activity against *Xanthomonas oryzae* pv. *oryzae* and *Alternaria* sp.

The antimicrobial activity of ZnONPs confirmed that these NPs could be employed effectively as a better agent for biomedical applications. In this respect, Steffy et al. [75] reported that ZnONPs act as a powerful antimicrobial agent against antibiotic-resistant bacterial pathogens, and for treating the non-healing ulcers. ZnONPs (with a size range of 10–12 nm) exhibited significant bactericidal efficiency against multidrug-resistant MDR-*E. coli*, MDR-*P. aeruginosa*, MDR-*Enterococcus faecalis* and Methicillin-resistant *S. aureus*. Furthermore, Hou et al. [76] reported that ZnONPs induced-bacterial cell-death against MDR-*Acinetobacter baumannii* that invading human lung cells without causing any obvious effect on the human lung cells viability. It was reported that ZnONPs have a potential antimicrobial activity against oral pathogens *Streptococcus mutans*, *Staphylococcus aureus* and *Enterococcus faecalis* and can be used as an alternative to the commercially available antimicrobial agents [77]. Also, the study performed by Quynh et al. [78] proved that ZnONPs performed a high antibacterial activity against *S. aureus* and *E. coli* up to 5 days that caused surgical site infection (SSI). Thus, fabricated ZnONPs were considered as a potent agent for efficient medical therapy.

6.1.1.1 Antimicrobial Activity Mechanism of ZnONPs It is proposed by many researchers that ZnONPs show their promising antimicrobial activities via several mechanisms. These NPs caused damage of the permeability of the plasma

membrane and loss of proton motive force. The release of Zn^{2+} ions has a significant inhibition of active transport, damage of the enzyme systems and amino acid metabolism. Furthermore, the oxidative stress of ZnONPs caused by the generation of reactive oxygen species (ROS) lead to the disturbance of mitochondrial functions and gene expression that lead to cell death [79].

One possible mechanism for the antimicrobial activity of ZnONPs is through the attachment of NPs to the microbial cell membrane via electrostatic forces. The positive zeta potential of ZnONPs promotes the attachment to the negatively charged microbial cell which leads to the penetration of ZnONPs into the cells. This interaction may damage the microbial cell integrity, resulting in the leakage of intracellular contents and ends with cell death [71]. In addition, Pati et al. [80] have shown that the disruption of the bacterial cell membrane integrity by ZnONPs caused a reduction of cell surface hydrophobicity, and down-regulation of the oxidative stress-resistance genes transcription in bacteria. To elucidate the mechanism of this action, Akbar and Anal [81] confirmed the disrupted cell membrane and accumulation of ZnONPs in the cytoplasm by using TEM and SEM images as well as FTIR, XRD analyses. Furthermore, Liang et al. [82] reported that FTIR analysis showed the binding of ZnONPs to polypeptides and glycogen from the *Streptococcus pyogenes* cell wall that lead to its disruption and cell damage.

The accumulation of ZnONPs in the outer membrane or cytoplasm of microbial cells triggers Zn^{2+} release. The released Zn^{2+} ions penetrate the cell membrane and disrupt the integrity of phospholipid bilayer in the microbial cell membrane. Disruption of the cell membrane is accompanied by the leakage of cytoplasmic contents like intracellular protein, genetic material, ATP and lipopolysaccharide. Moreover, free Zn^{2+} ions bind with the biomolecules such as proteins and carbohydrates, and subsequently damage the microbial cells [83].

Another possible mechanism for the antimicrobial activity of ZnONPs is based on the induced oxidative stress. The oxidative stress is formed in bacterial cell because of the interaction between Zn^{2+} ions and the thiol group of bacterial respiratory enzyme [84]. The formation of reactive oxygen species (ROS) such as superoxide anion (O_2^-), hydroxyl ion (OH^-) and hydrogen peroxide (H_2O_2) is a common antibacterial activity adopted by ZnONPs. It was reported that ROS damage the cellular components such as protein, lipid and nucleic acids. These free radicals could also turn down the mitochondrial functions and damage the electron transport chain and oxidative phosphorylation that resulting in microbial cell death. In addition, the increased oxidative stress initiates the gene expression to produce apoptotic markers and ultimately leads to cell death [85]. In the same manner, Mohd Yusof et al. [86] used SEM to examine the

morphological changes of the bacterial cells treated with ZnONPs. The findings suggested that ROS-induced oxidative stress caused membrane damage and bacterial cell death. Schematic illustration of the antimicrobial mechanism of ZnONPs against bacterial cells is presented in Fig. 1.

6.1.1.2 Factors Affecting the Antimicrobial Activity of ZnONPs The antimicrobial activity of ZnONPs is dependent upon their shape, size, concentration and the species of microbes.

6.1.1.3 Morphology of ZnONPs It was reported that the antimicrobial properties of ZnONPs depend on the morphology of NPs. Talebian et al. [87] found that flower-shaped ZnONPs exhibited more antimicrobial activity against *S. aureus* and *E. coli* than rod-shaped ZnONPs. In a similar work, Upadhyaya et al. [88] found that hexagonal ZnONPs displayed greater inhibition of *S. aureus* than rod-shaped. Khatami et al. [89] reported that the rectangular shaped ZnONPs at lower concentration had a higher antimicrobial effect against the same strains. In addition, Saif et al. [90] found that pyramid shaped ZnONPs exhibited the highest antimicrobial activity followed by hexagonal and then the round ones. Also, Sharma et al. [91] reported that the triangular ZnONPs showed better for antimicrobial activity against *Escherichia coli* and *Bacillus subtilis* as compared to the prototypical spherical counterparts. Overall, these observations suggest that sharp-edged ZnONPs may have greater antibacterial properties because they more easily penetrate the microbial cell wall than NPs with smooth edges that resulting in cell leakage and death.

6.1.1.4 Size of ZnONPs Previous reports revealed that by decreasing particle size, the antimicrobial activity of ZnONPs increases. The large surface area to volume ratio of NPs shows high antibacterial property, where it binds a greater number of ligands on its surface [92]. In this context, Jones et al. [93] confirmed that the antibacterial activity is mainly owing to smaller ZnONPs. They found that when the size of is 12 nm, it inhibits the growth of *S. aureus*, but when the size exceeds 100 nm, the inhibitory effect is minimal.

Also, Azam et al. [94] reported that the antimicrobial activity against both gram-positive (*S. aureus* and *Bacillus subtilis*) and gram-negative (*E. coli* and *P. aeruginosa*) bacteria increased with the decrease in particle size of ZnONPs. Moreover, Ohira and Yamamoto [95] indicated that from ICP-AES measurement, the amount of Zn^{2+} released from the small ZnONPs were much higher than the large ZnO powder sample. Similarly, Janaki et al. [96] showed that the formation of hydrogen peroxide is related to the size and surface area of synthesized NPs. Smaller the ZnONPs and larger the surface zone per unit area, the higher is the formation of oxygen species and hence, the hydrogen peroxide.

6.1.1.5 Concentration of ZnONPs The concentration of ZnONPs is considered as another factor affecting their antimicrobial activity. It was reported that the antimicrobial activity increases with increasing ZnONPs concentration [97]. Many previous studies have confirmed this conclusion. For instance, Elumalai and Velmurugan [98] indicated that the antimicrobial activity of ZnONPs against *S. aureus*, *B. subtilis*, *P. aeruginosa*, *P. mirabilis*, *E. coli*, *C. albicans* and *C. tropicalis* increased with increasing ZnONPs concentrations. Also, Rajeshkumar et al. [99] reported that ZnONPs exhibited substantial antibacterial, antifungal and antioxidant activities upon increasing their concentrations. In addition, Sumanth et al. [100] confirmed that ZnONPs produced by *Xylaria acuta* could proficiently exhibited antimicrobial and anticancer activities in a dose dependent manner.

6.1.1.6 Species of Microorganism In addition to the above mentioned factors affecting the antimicrobial properties of ZnONPs, microorganism species has reported as an additional important agent. Azam et al. [94] indicated that ZnONPs have shown maximum antimicrobial activity against *Bacillus subtilis* in comparison with other strains such as *E. coli* and *P. aeruginosa*. Also, Elumalai and Velmurugan [98] reported that *Staphylococcus aureus* bacterial strain was more susceptible to ZnONPs when compared to other bacterial and fungal strains such as *B. subtilis*, *P. aeruginosa*, *P. mirabilis*, *E. coli*, *C. albicans*, and *C. tropicalis*.

Velsankar et al. [101] found that *B. pumilus* was more sensitive to ZnONPs than *S. typhi*. In the same manner, Mohd Yusof et al. [86] indicated that ZnONPs synthesized by *Lactobacillus plantarum* TA₄, effectively inhibited the growth of *Staphylococcus aureus* compared to the other tested bacterial species (*Salmonella* spp. and *Escherichia coli*). These studies demonstrated that a lower concentration of ZnONPs displayed stronger antibacterial effects on Gram positive bacteria compared to the Gram-negative strains. This is likely due to differences in the composition of the cell wall between the two bacteria. The cell walls of Gram-positive bacteria contain peptidoglycan, teichoic acid, and abundant pores which allow foreign molecules and NPs to enter the cell, resulting in cell membrane damage and cell death. However, the cell walls of Gram-negative bacteria contain lipopolysaccharide, lipoprotein, and phospholipid, representing a barrier that only allows macromolecules to enter, hindering the entry of NPs and weakening the action of ZnONPs against Gram-negative bacteria [102].

6.1.2 Anticancer Activity of ZnONPs

Cancer is a conjunction of diseases characterized by the abnormal growth of tissue that might lead to the development of tumors that can spread into other tissues and cause severe effects in the patient, with complications

and severities potentially causing death [103]. Cancer was reported as the second cause of death in the US with approximately 2 million people being diagnosed every year [104]. Although applications of many protocols such as chemotherapy and radiotherapy are functional, these techniques have severe side effects, such as anemia, sickness, immunosuppression, or even death. In addition, some cancer cells have become resistant to such treatments, leading to the appearance of chemotherapy-resistant tumors [105]. As a consequence, significant efforts have been made towards to discover new approaches that overcome such drawbacks. Consequently, the use of nanotechnology has been reported to be applied towards cancer treatment [106]. The main advances of the NPs treatment are the direct effect on specific cancerous cells with no side effect on other cells and the efficient permeability to the tumor site, when compared to the free drugs [107].

ZnONPs exhibited a promising anticancer activity due to their good solubility, effective delivery to the cells, low toxicity, high biodegradability and biocompatibility [108]. Furthermore, ZnONPs are able to induce notable selective toxicity against cancer cells without damaging normal cells. That is because ZnONPs possess a unique electrostatic characteristic which helps in selecting targeting of cancer cells. Cancer cells contain anionic phospholipids on their surface which results in electrostatic attraction with ZnONPs, which promotes cellular uptake of ZnONPs by the cancer cells [109]. The mechanism behind the selective cytotoxicity of ZnONPs towards cancer cells is the intracellular release of dissolved zinc ions, followed by ROS induction. The production of ROS upon contact with the cells, lead to mitochondrial damage, reacted with the cell membrane lipids and resulted in the loss of protein activity balance, which induced cancer cell death via the apoptosis signaling pathway [110].

ZnONPs were able to target cancer cells and simultaneously perform several key functions, including inhibition of cancer proliferation, sensitization of drug-resistant cancer, prevention of cancer recurrence and metastasis, and resuscitation of cancer immune-surveillance [111]. In addition, because of their electrostatic properties, ZnONPs are rapidly taken up by the immune cells and thus can be used in combination with immunotherapy. In addition, the surface charge of these NPs is normally neutral but can be modulated depending on the pH; hence at biological conditions, ZnONPs are positively charged. This fact allows for their easy digestion by negatively-charged immune cells [112].

In the last few years, significant works have been achieved concerning the great potential of using ZnONPs as a nanomedicine agent. For instance, Shilpa et al. [113] reported that by the application of ZnONPs, the proliferation of human breast cancer (MCF7) cells was substantially reduced when compared with the viability control cells. Also, Dutta et al.

[66] reported that the green synthesized ZnONPs showed a remarkable selective cytotoxicity against the Human Cervical cancer (HeLa) and Human colon cancer (HT-29) cell lines.

Based on the MTT assay, Aldabahi et al. [114] demonstrated a potent cytotoxic effect of the ZnONPs against the HeLa cancer cell line. Bhattacharya et al. [115] indicated a great reduction in the viability of skin melanoma (B16F10) cells exposed to ZnONPs in a dose dependent manner. In addition, cellular viability (ED_{50}) was recorded for ZnONPs at 3% dose while commercial ZnO exhibited ED_{50} at 6% dose. Parthasarathy et al. [116] reported that ZnONPs synthesized by *Bacillus cereus* PMSS-1 exhibited concentration-dependent cytotoxicity on human melanoma A375 cells. ZnONPs induced the apoptosis of the cells as evidenced by the increased lipid peroxidation (LPO), diminished activities of antioxidants such as superoxide dismutase (SOD), catalase (CAT) and glutathione peroxidase (GPx). Moreover, the administration of ZnONPs increased ROS production and reduced mitochondrial membrane potential (MMP) in A375 cells. Therefore, ZnONPs could be used for human malignant melanoma after proper in vivo studies.

ZnONPs synthesized by *Alternaria tenuissima* inhibited the proliferation of normal human melanocytes, human breast and liver cancer cell lines with IC_{50} concentrations of 55.76, 18.02 and 16.87 $\mu\text{g}/\text{ml}$, respectively [117]. In the same line, Manimaran et al. [118] investigated the in vitro cytotoxicity assay that depicted a significant level of cytotoxic effects of ZnONPs synthesized by *Pleurotus djamor* against the A549 lung cancer cells with LC_{50} values 42.26 $\mu\text{g}/\text{ml}$. The anticancer activity of ZnONPs in different cancer types is presented in Table 3. The study of Housseiny and Gomaa [119] provided an insight on using γ -radiation as a highly efficient and inexpensive tool for the enhancement of antitumor effects of NPs against tumor diseases. Samples of ZnONPs produced by *Penicillium chrysogenum* exposed to 20 kGy dose recorded the greatest antitumor effect. The IC_{50} values of human breast carcinoma (MCF-7) were 373 $\mu\text{g}/\text{ml}$ and $> 500 \mu\text{g}/\text{ml}$, while of colon carcinoma cells (HCT-116) were 226 and 317 $\mu\text{g}/\text{ml}$ for irradiated and non irradiated samples, respectively. The in vitro assay showed that the biogenic ZnONPs displayed high cytotoxicity with IC_{50} value of $4.04 \times 10^{-1} \mu\text{g}/\text{ml}$ when exposed to human liver by the modulation of proliferation and inducing apoptosis [120]. The overall findings of the previous studies suggested that the microbial synthesized ZnONPs could act as an alternative biomedical agent for future cancer therapeutic protocols.

6.1.3 Anti-inflammatory Activity of ZnONPs

Inflammation is the host body response in response to physical and chemical stress or injury in order to restore cellular

Table 3 The anticancer effects of microbial synthesized ZnONPs in different human cancer cell lines

Microorganism produced	Targeted cell line	Effect and mechanism	References
<i>Rhodococcus pyridinivorans</i>	HT-29, colon	ZnONPs suppressed cell viability in Caco-2 cell line via increased ROS and induced IL-8 release ZnO NPs and fatty acids could induce lysosomal destabilization in Caco-2 cells	[189, 207, 208]
<i>Aspergillus niger</i>	HepG2, liver	ZnONPs caused ROS generation and oxidative DNA damage and lead to mitochondrial-mediated apoptosis in HepG2 cells ZnONPs selectively induce apoptosis in HepG2 cells, which was also mediated by ROS via the p53 pathway	[28, 209, 210]
<i>Aspergillus niger</i>	A549, lung	ZnONPs incorporated in liposomes not only rendered pH responsivity to the delivery carrier but also exhibited synergetic chemo-photodynamic anticancer action	[211, 212]
<i>Aspergillus terreus</i>	MCF-7, breast	Ecofriendly formulated ZnONPs arrest the cell cycle in the G2/M phase and upregulated proapoptotic genes p53, p21, Bax, and JNK and downregulated antiapoptotic genes Bcl-2, AKT1, and ERK1/2 in a dose-dependent manner in MCF-7 cells	[213]
<i>Penicillium chrysogenum</i>	MCF-7, breast HCT-116, colon	A doxorubicin delivery system based on zinc oxide nanomaterials can bypass the P-gp increase in the drug accumulation in resistant MCF-7R and MCF-7S cells ZnO NPs induced Caco-2 cells cytotoxicity associated with increased intracellular Zn ions	[119, 214, 215]
<i>Pichia kudriavzevii</i>	MCF-7, breast	RGD (Arg-Gly-Asp)-targeted ZnO NPs can target integrin $\alpha v \beta 3$ receptors to increase the toxicity of the ZnO NPs to MDA-MB-231 cells at lower doses	[216]

homeostasis and tissue microenvironment [121]. Non-steroidal anti-inflammatory drugs (NSAIDs) commercially available in the market show some limitations such as gastric ulcers, renal issues and cardiovascular strokes [122]. The development of NPs opens a new therapeutic window for the management of inflammation-based disorders [123].

It was reported that ZnONPs are broadly used as an anti-inflammatory agent. They exert their anti-inflammatory activity through various mechanisms, namely, inhibition of myeloperoxidase, proinflammatory cytokine release, nuclear factor kappa B (NF- κ B) pathway, mast cell degranulation inducible nitric oxide synthase enzyme (iNOS) and hence down regulation of nitric oxide (NO) release [124]. Moreover, a significant inhibition of bovine serum albumin (BSA) protein denaturation of ZnONPs evidenced their anti-inflammatory property [125].

It was demonstrated that ZnONPs had great effects on reducing skin inflammation in Atopic dermatitis (AD) models. ZnONPs with a small size were able to reach into the deep layers of the allergic skin and exerted higher anti-inflammatory properties by decreasing drastically on pro-inflammatory cytokines in the mouse model of AD [126]. The anti-inflammatory activity of ZnONPs is not confined to atopic dermatitis treatment, but has also shown to be very effective for other inflammatory diseases. The anti-inflammatory activities of ZnONPs in LPS-stimulated RAW 264.7 macrophages were investigated. ZnONPs exposed remarkable anti-inflammatory activity by dose-dependently suppressing NO production as well as the related protein

expressions of iNOS, COX-2, IL-1 β , IL-6, and TNF- α . Hence, ZnONPs have the potential to be utilized for anti-inflammatory treatments [127].

6.1.4 Wound Healing Activity of ZnONPs

Skin is the largest organ of our body which protects us from external invasion and any damage happened to the skin results in a wound. Wound healing is an active process, where replacement of injured tissue to its initial state exactly after the injury and the depletion of injured area in a clear-cut indication of healing [14]. However, wound healing may delay due to microbial infection. In particular, *Staphylococcus aureus* and *Pseudomonas aeruginosa* are from microorganisms which cause severe wound infections. Metal oxide NPs can enhance the process of wound healing due to their antimicrobial activity against these pathogenic organisms [75].

The wound healing activity effect of ZnONPs has reported due to their marked antimicrobial activity, low cost and remarkable thermostability [54]. In addition, it was found that wound healing is impaired with zinc deficiency. So, ZnONPs can be used as a therapeutic approach to enhance the rate of wound healing [20]. Several literatures evidenced the use of ZnONPs as a successful wound healing agent. For instance, Shao et al. developed a gel using ZnONPs which showed remarkable wound healing property in rats and thus proved to be an efficient topical antimicrobial formulation and wound healing agent [128]. In a

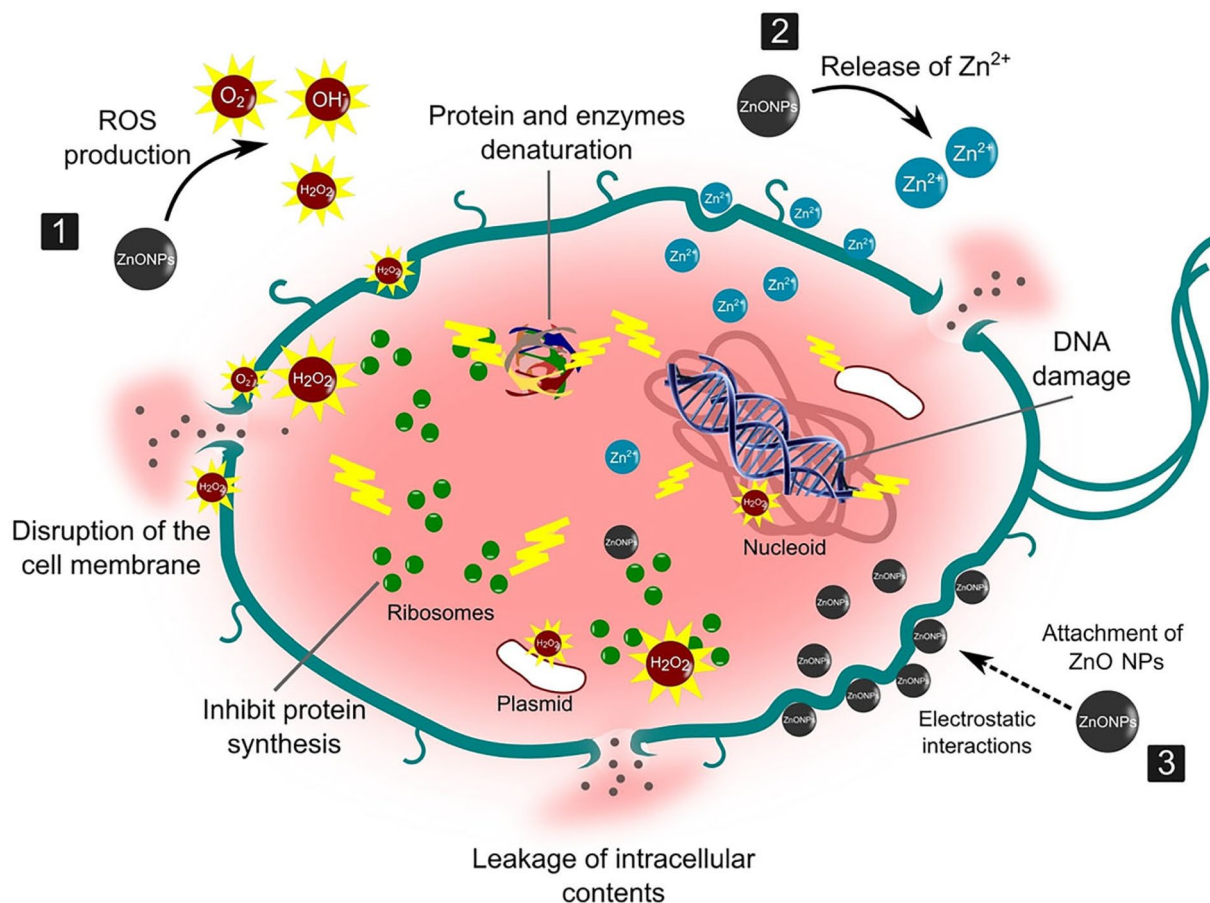


Fig. 1 Schematic illustration of the antimicrobial mechanism of ZnONPs against bacterial cells. ZnONPs act as an antimicrobial agent through the following mechanisms: (1) the formation of reactive oxygen species (ROS), which induces oxidative stress and membrane and DNA damage, resulting in bacterial death; (2) dissolution

of ZnONPs into Zn^{2+} , which interferes with enzyme, amino acid, and protein metabolisms in bacterial cells; and (3) direct interaction between ZnONPs and cell membrane through electrostatic forces that damages the membrane plasma and causes intracellular content leaks

similar study, the cotton wound bandages impregnated with ZnONPs give patches with antimicrobial properties. This property can potentially be used for treating and covering infection-sensitive wounds, namely diabetic or burn wounds [89].

The study of Ezealisiji et al. [129] suggested that there is a need to investigate the optimum dose of ZnONPs and the necessary time required for providing of the optimum conditions for their application. In the same line, it was reported that wound contraction is caused by activity of myofibroblasts which reduces wound area. The hydrogel based wound dressing integrates in increasing contact time and further follows keratinocyte migration and enhances re-epithelialization [130]. The mechanism by which ZnONPs heals the burn wound is a complex interplay between intracellular and extracellular agents and poses a potential reflex to use them in order to treat burn wound safely and effectively. ZnONPs dressing increases apoptosis, bacterial clearance, platelet activation, tissue necrosis, re-epithelialization, tissue scar

formation, debris removal, angiogenesis and stem cell activation through wound healing [131].

It is well known that, there is an intimate association of wound healing, inflammation and immune response. Thus, ZnONPs enhance the skin re-epithelization via its anti-inflammatory action due to suppression of inflammatory marker genes like IL-6, IL-1 β , IL-10, and TNF- α [127]. In addition, proficently zinc enhances platelet activity and aggregation [132]. Zinc mediates its effect on platelets Protein kinase C (PKC)—mediated tyrosine phosphorylation of platelet proteins. The platelets are being able to be recognized as immune cells capable of pathogen recognition via cytokines and chemokines [133]. Both precursor and mature B-cells can reduce antibody production if zinc is deficient at the site of the wound. Wound clearance gets hindered due to falling B-cells populations and circulating antibodies that would negatively affect phagocytosis. ROS-mediated augmentation of human dermal fibroblast migration is one of the hallmark actions of zinc [134].

6.2 Agricultural Applications of ZnONPs

Agriculture is the backbone of the third world economy, but unfortunately now, the agriculture sector undergoes various global challenges like climate changes, urbanization, and sustainable use of resources. Furthermore, the accumulation of fertilizers and pesticides represents another environmental factor. On the other side, human population is increasing daily and food demand is growing rapidly, so there is an urgent to adopt efficient techniques to make agriculture more sustainable [135]. In this respect, NPs have been reported to be a promising strategy to enhance plant growth and productivity due to their unique properties such as high surface area/volume ratio, high adsorption, high catalytic activity, large number of reactive sites, and high chemical stability as compared to bulk ion [136]. ZnONPs may find use in agriculture in the form of nanofertilizers, growth regulators, or as nanopesticides to address plant and zoonotic diseases [137]. The application of ZnONPs as a fertilizer, in salinity and drought mitigations has been reviewed.

6.2.1 ZnONPs as a Fertilizer

ZnONPs with unique physiochemical properties may serve as a potent fertilizer for the improvement of crop yield and food quality. For instance, Moghaddasi et al. [138] reported that the treatment of *Cucumis sativus* with ZnONPs (1 mg/l) showed increasing in the biomass and length of shoot and root as compared to bulk ZnO. In the same line, Rameshraddy et al. [139] reported that the plant height, chlorophyll content, biomass and Zn content in leaf and seed were higher in rice samples treated with ZnONPs compared to Zn fertilizer (ZnSO_4). Moreover, Tiwari [140] found that seed treatment of maize plant with ZnONPs at the concentration of 500 to 2000 ppm resulted in higher seed vigor, forage and grain yields as well as higher zinc content.

The application of ZnONPs at 0.50 ml/l caused a greater increase in plant length, carotenoids, H_2O_2 , chlorophyll, SOD, CAT, APX, PAL, proline and GSH contents. The possible reason for enhanced photosynthesis is due to an improvement in carbonic anhydrase, which could have facilitated the supply of CO_2 to the sites of carboxylation in the chloroplast [141]. In the same line, Singh et al. [9] reported that ZnONPs at the concentration of 50 ppm was the optimum concentration for increasing rice seedling growth and improving of physiological processes.

Bala et al. [142] reported that foliar application of ZnONPs at the concentrations of 500 to 5000 ppm of increased growth and yield indices (height of shoot and root fresh and dry weights) in *Oryza sativa* plants. In addition, Garcia-Lopez et al. [143] indicated that using 1000 ppm concentration of ZnONPs increased stem diameter, chlorophyll content, fruit yield, and total biomass in habanero

pepper plant. Seydmohammadi et al. [144] found that foliar application of ZnONPs (6 mg/l) increased the number of leaves and lateral branches, leaf chlorophyll and petal anthocyanin contents as well as the number of flowers. Likewise, Shahhoseini et al. [145] reported that application of ZnONPs increased the biological yield, essential oil content, and Zn absorption of Feverfew. In the same respect, Sadak and Bakry [146] indicated that the application of ZnONPs increased free amino acids, proline, and total carbohydrates of straw plant. In addition, the application of these NPs was effective for photosynthetic pigments content, fresh and dry weights of shoot and root systems.

6.2.2 ZnONPs in Salinity Tolerance

In addition to their applications as a potent fertilizer for the improvement of crop yield, ZnONPs have been reported to be used for salinity tolerance in the plants. In this respect, Torabian et al. [147] reported higher shoot dry weight, proline content, and some antioxidant enzyme activities of sunflower cultivars upon the treatment with ZnONPs under salinity stress. The small size of such NPs leads to high mobility and thus rapid transport of the nutrient to all parts of the plant. Also, Alharby et al. [148] proved that ZnONPs alter mRNA expression of SOD and GPX genes, and proteins in tomato (*Lycopersicon esculentum* Mill.) plant subjected to NaCl stress. In addition, the treatment of lupine plants (*Lupinus termis*) with ZnONPs at the concentration of 60 mg/l under salinity stress (150 mM NaCl) stimulated growth, promoted the formation of photosynthetic pigments, phenolic compounds and ascorbic acid. The treatment of the plants with ZnONPs increased the activity of superoxide dismutase, catalase and other antioxidant enzymes [149].

Vojodi Mehrabani et al. [150] showed a promising effect on elemental content (K^+ , Na^+ and Zn^{2+}), soluble sugars content, flavonoids, H_2O_2 and MDA contents as well as the essential oil yield of *Rosmarinus officinalis* plant under salinity stress upon treatment with ZnONPs. Also, Hussein and Abou-Baker [151] found that the foliar application of ZnONPs (200 ppm) led to mitigating the adverse effect of salinity and confirmed that diluted seawater could be used in the irrigation of the cotton plant. Wang et al. [152] reported that the treatment of the wheat plant with ZnONPs caused the reduction of sodium concentration and increasing the photosynthetic rate. The application of these NPs enhanced the activity of various some antioxidant enzymes like SOD, APX and CAT. In addition, Noohpisheh et al. [153] studied the effects of ZnONPs under salinity stress in two cultivars of *Trigonella foenum-graecum* and reported that the effects are cultivar and salinity dependent. The application of these NPs increased the concentration of calcium of root in one cultivar where it decreased in the other. In addition ZnONPs

increased the proline content and trigonelline content under salinity and normal conditions.

6.2.3 ZnONPs in Drought Tolerance

ZnONPs have been also reported to be used in drought mitigation in the plants. In this respect, Taran et al. [154] showed that ZnONPs decreased the negative effect of drought action on wheat seedling by increasing the activity of antioxidative enzymes and the relative water content in the leaves. These NPs also reduced the level of accumulation of thiobarbituric acid reactive substances (TBARS) and stabilized the content of photosynthetic pigments. Moreover, Rameshraddy et al. [139] reported that rice plants treated with ZnONPs (1000 mg/l) showed drought tolerance via maintaining the membrane stability and higher expression of Cu/Zn SOD. Additionally, these NPs improved plant height, chlorophyll content, biomass, tiller number, and yield of the plant under drought stress.

Dimkpa et al. [155] confirmed that ZnONPs could alleviate the harmful effects of drought in sorghum. The application of ZnONPs improved grain yield (22–183%) under drought stress. Dhalimi and Ajeel [156] confirmed that under drought stress, foliar application of ZnONPs to sunflower (*Helianthus annuus* L.) increased the level of auxin (IAA), Gibberline (GA3) and leaf content of zinc. In the same line, Sun et al. [157] found that the application of ZnONPs promote the drought tolerance in maize. These NPs alleviated the photosynthetic pigments degradation, enhanced water use efficiency and maintained a higher photosynthetic rate.

6.3 Environmental Applications of ZnONPs

Water is the most valued and important resource in the world and its lack become a serious problem. However some factors such as climate changes, textile paints and non-biodegradable dyes result in the accumulation of organic wastages and contamination of water. It causes many diseases such as diarrhea, typhoid, fever, dysentery, cholera and thus resulting in death [158]. Thus, water purification become an urgent demand for human health.

Water purification can be performed by traditional methods that include filtration, coagulation, solvent extraction, precipitation, adsorption, ion exchange, floatation, oxidation, ozonation, catalytic degradation and biological treatment [159]. However, there are many restrictions and limitations that make the search of new alternatives become necessary. Among these methods, nanomaterials have gained tremendous attention in recent years due to their high efficiency, high surface reactivity, and broad application for several environmental purposes [160]. The application of ZnONPs has received significant attention for water treatment because of their nontoxicity, long-term stability, low

cost, biocompatibility and effective surface properties [161]. ZnONPs play an efficient role in the wastewater industry as a photocatalyst and can degrade dyes and different types of organic matter. In this context, Rajendran and Sengodan [162] indicated that ZnONPs act as a potential photocatalyst to remove the organic pollutant present in seafood industry during effluent treatment.

The irradiation of ZnONPs by sunlight and having a high photonic energy result in the excitation of electrons to the empty conduction band producing electron–hole pairs which migrate to ZnONPs surfaces and undergo oxidation/reduction where H^+ reacts with water molecules and OH^- forming OH^\bullet (hydroxyl radicals). The electrons upon reacting with oxygen produce superoxide free radical anions resulting in the formation of hydrogen peroxide that reacts further with superoxide radicals to form OH radicals. The resulting OH radicals are strong oxidizing agents that react with organic and inorganic pollutant absorbed on the surface of ZnO to produce intermediate compounds and convert to green compounds i.e. H_2O , CO_2 and inorganic compounds [163].

The microbial synthesized ZnONPs can be effectively used in the decontamination of fluoride from waste water. The study of Shabnam et al. [164] stated that the absorption of fluoride is achieved up to 65% from waste water using ZnONPs. Furthermore, ZnONPs showed good photocatalytic activity when used for the degradation and treatment of several dyes such as methylene blue, methyl orange, methyl red, congo red, acid Blue 9 and Coomassie Brilliant Blue R-250 and reactive red dyes [165, 166]. In this context, Bhuyan et al. [167] indicated that upon addition of ZnONPs as a photocatalyst, the concentration of methylene blue dye decreased by 50% after 30 min. At the end of the reaction (180 min), it was observed that methylene blue dye degraded from 82% of its initial value. Also, Nava et al. [168] reported that the photocatalytic degradation of methylene blue under UV illumination after 180 min showed that ZnONPs exhibited maximum photodegradation percentage (97%). Likewise, Vinayagam et al. [163] showed that ZnONPs could efficiently degrade more than 88% of methylene blue dye within 270 min. Also, Raghavendra et al. [68] reported that the biosynthesized ZnONPs exhibited great photodegradation of Methylene Blue, Rhodamine-B and Nigrosine dyes under sunlight irradiation at different time intervals. Furthermore, the decolorization percentages of the methylene blue and Eosin Y dyes were 84% and 94%, respectively, which indicate an efficient degradation of the ZnONPs [114].

ZnONPs also exhibited strong photodegradation activity of methyl orange dye that used as a model pollutant and caused a great environmental pollution [169]. In this regard, Karnan and Selvakumar [170] reported that under sunlight, ZnONPs exhibited around 83.99% decolorization efficiency of methyl orange dye at 120 min. In the study of Jain et al. [74], after 80 min, ~90% of methyl orange degradation

was observed by ZnONPs synthesized by *Serratia nematodiphila*. Moreover, the synthesized ZnONPs were used as nanocatalyst for photodegradation of reactive red 195 and methyl orange as anionic dyes utilizing UV light irradiation. The degradation of reactive red 195 dye was 91–94% after 70 min over the synthesized zinc oxide and the values of degradation increased to be 99–99.8% in 50 min with H₂O₂ under UV light irradiation [171]. Therefore, these findings confirmed an effective approach to utilize ZnONPs as an efficient photocatalyst agent.

7 Toxicological Effects of ZnONPs

ZnONPs are the most commonly used NPs due to its varied applications ranging from personal care products, sensors, antibacterial creams and biomedical applications. These numerous applications in various fields have aroused the need for the investigation of the possible toxic effects of ZnONPs [172]. Furthermore, the unique properties of these NPs make them highly reactive upon their exposure to biological systems [173]. Thus, it is a necessary to investigate the toxic effect of ZnONPs on plants, animals and hence human health.

The NPs toxicity on plant growth, metabolism, defense system, and yield may depend on the route of exposure, media composition, dose, particle morphology (size, shape), particle composition, and surface chemistry [174]. In this respect, Yusefi-Tanha et al. [175] investigated the potential phytotoxicity of ZnONPs on soil-grown soybean (*Glycine max* CV. Kowsar) during its lifecycle. The results demonstrated a significant influence of ZnONPs on seed yield, lipid peroxidation, and various antioxidant biomarkers in soybean. It was also suggested differential nano-specific toxicity of ZnONPs compared to the ionic Zn²⁺ toxicity in soybean. The results indicated the potential of ZnONPs to be used as a nanofertilizer for crops grown in Zn-deficient soils to improve crop yield, food quality and address malnutrition, globally. However, other authors reported that when ZnONPs and their derivatives are available in soil in excess, potential toxicity may result in plants, including inhibitory effects on seed germination, growth, photosynthesis, physiological and biochemical traits, yield characteristics, and nutritional quality [176].

Nevertheless, studies have suggested that the toxicity effects of ZnONPs are dependent on their concentration (dose), size, morphology, and surface composition [177]. In this respect, oral administration of ZnONPs (20 mg/kg body weight) in lambs increased the levels of blood urea nitrogen (BUN) and creatinine, indicating renal dysfunction [178]. In the histopathological examination, a high concentration of oral administration of ZnONPs at 400 mg/kg induced focal hemorrhages and necrosis of the liver and

heart tissue of Wistar rats, which were caused by oxidative stress [179]. Furthermore, Wang et al. [180] found that the supplementation of high doses of ZnONPs (5000 mg/kg body weight) caused a great toxicity in mice by decreasing the body weight and increasing the relative weight of the pancreas, brain, and lung. Moreover, zinc accumulation was observed in the liver, pancreas, kidney and bones.

Concerning the effect of the size and morphology of the ZnONPs on their toxicity, it was reported that bigger NPs also tend to stay longer in the kidneys due to the slower excretion mechanisms of glomerular filtration and this long-term retention can lead to organ toxicity [181]. Furthermore, different morphologies of NPs also contribute to their toxicity. In this respect, Wahab et al. [182] investigated the cytotoxicity effects of ZnONPs with different morphologies such as nanoplates, nanorods, nanosheet, and nanoflower on malignant human T98G gliomas and fibroblast cells. Nanorods demonstrated higher cytotoxicity and inhibitory effects on cancer and normal cells, respectively. This may be due to a larger effective surface area that potentially induces higher oxidative stress on cells.

The toxicity mechanisms of ZnONPs still remain unclear. However, it has been proposed that three noteworthy toxicity activities of ZnONPs are reported. These include the direct contact of ZnONPs with the cells, release of zinc ions (Zn²⁺) from ZnONPs and production of ROS [12]. The contact of ZnONPs with cells cause mechanical harm like a change in cell morphology, distortion of membranes, complication or spillage of intracellular structures, mitochondrial harm and outflow of specific organelles. The released zinc ions (Zn²⁺) prompt mitochondrial damage and disrupt cellular zinc homeostasis that prompting potential damage of the cells [183]. When ZnONPs enter inside the cell, the cellular defence mechanism begins to create ROS. The presence of ROS causes cytokines promoting inflammation. This inflammation generates oxidative stress-mediated DNA damage and lipid peroxidation, which subsequently cause apoptosis [184].

Overall, in order to better understand the therapeutic benefits and avoid unintended cytotoxic effects and clinical diagnostic potential, a future research studies are needed in both in vitro and in vivo to address the dose and duration of exposure required for causing the potential toxic effects of ZnONPs. Furthermore, the long-term consequences still have to be studied for better and safe usage of these NPs.

8 Conclusion

ZnONPs have gained significant interest due to their unique physicochemical properties and the wide applications in diverse areas. The microbial synthesis methods of ZnONPs has recently gained much importance because it is simple,

cheap, biocompatible, eco-friendly and easily scaled up compared to other physical and chemical methods. ZnONPs are considered as a potential platform for biomedical research due to their antimicrobial, anticancer, anti-inflammatory, and wound healing activities. In the agriculture field, ZnONPs could be used as a nanofertilizer agent and for the tolerance of the salinity and drought harm. In addition, ZnONPs with unique photocatalytic potential can effectively use for degradation of harmful dyes and other chemicals present in water. However, more research should be done for the evaluation of novel groups of microbes and optimization of the synthesis process. Furthermore, more investigations for their toxicity toward biological systems remain a controversial issue in recent researches.

Author Contributions EZG contributed to the design and implementation of the research, the analysis of the results, and the writing of the manuscript.

Funding Open access funding provided by The Science, Technology & Innovation Funding Authority (STDF) in cooperation with The Egyptian Knowledge Bank (EKB). Not applicable.

Declarations

Conflict of interest The author declares that they have no conflict of interest.

Research Involving Human Participants or Animals This article does not contain any studies with human participants or animals performed by any of the author.

Ethical Approval Not applicable.

Consent to Participate Not applicable.

Consent for Publication Not applicable.

Availability of data and materials Data are available upon request from the author.

Open Access This article is licensed under a Creative Commons Attribution 4.0 International License, which permits use, sharing, adaptation, distribution and reproduction in any medium or format, as long as you give appropriate credit to the original author(s) and the source, provide a link to the Creative Commons licence, and indicate if changes were made. The images or other third party material in this article are included in the article's Creative Commons licence, unless indicated otherwise in a credit line to the material. If material is not included in the article's Creative Commons licence and your intended use is not permitted by statutory regulation or exceeds the permitted use, you will need to obtain permission directly from the copyright holder. To view a copy of this licence, visit <http://creativecommons.org/licenses/by/4.0/>.

References

1. S. Mustapha, M.M. Ndamitso, A.S. Abdulkareem, J.O. Tijani, D.T. Shuaib, A.O. Ajala, A.K. Mohammed, *Appl. Water Sci.* **10**, 49–61 (2020)
2. S. Marimuthu, A.J. Antonisamy, S. Malayandi, K. Rajendran, P.C. Tsai, A. Pugazhendhi et al., *J. Photochem. Photobiol. B* **205**, 111823 (2020)
3. A. Mahvash, A. Javadi, H. Jafarizadeh-Malmiri, *Green Process Synthesis* **9**(1), 375–385 (2020)
4. F. Malek, M. Nahid, *J. Nanostructure Chem.* **8**, 93–102 (2018)
5. M. Saravanan, V. Gopinath, M.K. Chaurasia, A. Syed, F. Ameen, N. Purushothaman, *Microb. Pathog.* **115**, 57–63 (2018)
6. S.S. Roshitha, V. Mithra, V. Saravanan, S.K. Sadasivam, M. Gnanadesigan, *Biores. Technol. Rep.* **5**, 339–342 (2019)
7. J.N. Hasnidawani, H.N. Azlina, H. Norita, N.N. Bonnia, *Proced Chem.* **19**, 211–216 (2016)
8. R. Suntako, *Bull Mater Sci.* **38**, 1033–1038 (2015)
9. A. Singh, N.B. Singh, S. Afzal, T. Singh, I. Hussain, *J. Material. Sci.* **53**, 185–201 (2018)
10. R. Bharathi, A. Rajasekar, S. Rajeshkumar, *Plant Cell Biotechnol. Mol. Biol.* **21**, 58–64 (2020)
11. R. Akshaya, S. Rajeshkumar, A. Roy, T. Lakshmi, *Int. J. Res. Pharm. Sci.* **11**(4), 5269–5273 (2020)
12. A. Król, P. Pomastowski, K. Rafińska, V. Railean-Plugaru, B. Buszewski, *Adv. Colloid. Interface Sci.* **249**, 37–52 (2017)
13. H.S. Agarwal Menon, S. Venkat Kumar, S. Rajeshkumar, *Chem. Biol. Interact.* **286**, 60–70 (2018)
14. A. Khalid, R. Khan, M. Ul-Islam, T. Khan, F. Wahid, *Carbohydr. Polym.* **164**, 214–221 (2017)
15. P. Singh, Y.J. Kim, D. Zhang, D.C. Yang, *Trend Biotechnol.* **34**, 588–599 (2016)
16. A. Gour, N.K. Jain, *Artif. Cells Nanomed. Biotechnol.* **47**, 844–851 (2019)
17. A. Raja, S. Ashokkumar, R. Pavithra Marthandam, J. Jayachandiran, C.P. Khatiwada, K. Kaviyarasu, R. Ganapathi Raman, M. Swaminathan, *J. Photochem. Photobiol. B* **181**, 53–58 (2018)
18. I. Pócsi, In: Banfalvi G, ed. Springer Netherlands. (2011) 31–58.
19. P. Dhandapani, A.S. Siddarth, S. Kamalasekaran, S. Maruthamuthu, G. Rajagopal, *Carbohydr. Polym.* **103**, 448–455 (2014)
20. D. Medina Cruz, G. Mi, T.J. Webster, *J. Biomed. Mater. Res. A* **106**, 1400–1412 (2018)
21. E. Selvarajan, V. Mohanasrinivasan, *Mater. Lett.* **112**, 180–182 (2013)
22. R.M. Tripathi, A.S. Bhadwal, R.K. Gupta, P. Singh, A. Shrivastav, B.R. Shrivastav, *J. Photochem. Photobiol. B* **141**, 288–295 (2014)
23. M. Abinaya, B. Vaseeharan, M. Divya, A. Sharmili, N.S. Marimuthu Govindarajan, S.K. Alharbi, J.M. Khaled, G. Benelli, *J. Trace Elem. Med. Biol.* **45**, 93–103 (2018)
24. M. Sastry, A. Ahmad, M. Islam Khan, R. Kumar, *Curr. Sci.* **85**, 162–170 (2003)
25. M. Kitching, M. Ramani, E. Marsili, *Microb. Biotechnol.* **8**, 904–917 (2015)
26. A. Zielonka, M. Klimek-ochab, *Adv. Nat. Sci. Nanosci. Nanotechnol.* **8**, 1–9 (2017)
27. K.V. Pavani, N. Sunil Kumar, B.B. Sangameswaran, *Polish J. Microbiol.* **6**, 161–163 (2012)
28. Y. Gao, M.A. Vijaya Anand, V. Ramachandran, V. Karthikkumar, V. Shalini, S. Vijayalakshmi, D. Ernest, *J. Clust. Sci.* **30**, 937–946 (2019)
29. M.A. Rauf, M. Owais, R. Rajpoot, F. Ahmad, N. Khan, S. Zubair, *RSC Adv.* **7**, 36361–36373 (2017)

30. N.I. Hulkoti, T.C. Taranath, *Colloids Surf. B* **121**, 474–483 (2014)
31. N. Jain, A. Bhargava, J.C. Tarafdar, S.K. Singh, J. Panwar, *Appl. Microbiol. Biotechnol.* **97**, 859–869 (2013)
32. V.N. Kalpana, B.A.S. Kataru, N. Sravani, T. Vigneshwari, A. Panneerselvam, V. Devi Rajeswari, *OpenNano* **3**, 48–55 (2018)
33. Y.N. Slavin, J. Asnis, U.O. Häfeli, H. Bach, *J. Nanobiotechnol.* **15**, 65 (2017)
34. S. Irvani, *Int. Sch. Res. Notes* **2014**, 1–18 (2014)
35. Z. Molnár, V. Bóday, G. Szakacs, B. Erdélyi, Z. Fogarassy, G. Sáfrán, T. Varga, Z. Kónya, E. Tóth-Szeles, R. Szucs, I. Lagzi, *Sci. Rep.* **8**, 1–12 (2018)
36. A. Verma, M.S. Mehata, *J. Radiat. Res. Appl. Sci.* **9**, 109–115 (2016)
37. S. Nagarajan, K.A. Kuppusamy, *Ind. J. Nanobiotechnol.* **11**, 39 (2013)
38. N. Bala, S. Saha, M. Chakraborty, M. Maiti, S. Das, R. Basu, P. Nandy, *RSC Adv.* **5**, 4993–5003 (2015)
39. P. Dhadapani, A.S. Siddarth, S. Kamalasekaran, S. Maruthamuthu, G. Rajagopal, *Carbohydr. Polym.* **103**, 448–455 (2014)
40. A. Bhargava, N. Jain, M.A. Khan, V. Pareek, R.V. Dilip, J. Panwar, *J. Environ. Manag.* **183**, 22–32 (2016)
41. C. Chinnasamy, P. Tamilselvam, B. Karthick, B. Sidharth, M. Senthilnathan, *Mater Today Proc.* **5**, 6728–6735 (2018)
42. P. Jamdagni, P. Khatri, J.S. Rana, *J. King Saud. Univ. Sci.* **30**(2), 168–175 (2018)
43. A.B. Moghaddam, M. Moniri, S. Azizi, R.A. Rahim, A.B. Ariff, W.Z. Saad et al., *Molecules* **22**, 1–18 (2017)
44. J. Vaishnav, V. Subha, S. Kirubanandan, M. Arulmozhi, S. Renganthan, *J. Optoelectron. Biomed. Material.* **9**(1), 59–71 (2017)
45. F.S. Rocha, A.J. Gomes, C.N. Lunardi, S. Kaliaguine, G.S. Patience, *Can. J. Chem. Eng.* **96**, 2512–2517 (2018)
46. H. Chandra, D. Patel, P. Kumari, J.S. Jangwan, S. Yadav, *Mat. Sci. Engin. C* **102**, 212–220 (2019)
47. M. Faraldos, and A. Bahamonde, *Materials*, Elsevier Ltd. <https://doi.org/https://doi.org/10.1016/B978-0-08-102641-0.00023-2> (2018).
48. M.M. Modena, B. Rühle, T.P. Burg, S. Wuttke, *Adv. Mater* **31**, 1–26 (2019)
49. P. Senthil Kumar, K. Grace Pavithra, and M. Naushad, Elsevier Inc. <https://doi.org/https://doi.org/10.1016/B978-0-12-813337-8.00004-7> (2019).
50. C. Parthiban, N. Sundaramurthy, *Int. J. Innov. Res. Sci. Engin. Technol.* **4**(10), 9710–9718 (2015)
51. C. Jose Chirayil, J. Abraham, R. Kumar Mishra, S.C. George, and S. Thomas, (2017) 1–36.
52. T. Abbasi, J. Anuradha, S.U. Ganaie, S.R. Khandelwal, *Colloids Surf. B* **4**, 194–198 (2013)
53. A.A. Bunaciu, E. Udriștioiu, H.Y. Aboul-Enein, *Crit. Rev. Anal. Chem.* **45**, 289–299 (2015)
54. H.N. Kumar, N.C. Mohana, B.R. Nuthan, K.P. Ramesha, D. Rakshith, N. Geetha, S. Satish, *SN Appl. Sci.* **1**(6), 651 (2019)
55. W.H. Qi, M.P. Wang, *J. Nanoparticle Res.* **7**, 51–57 (2005)
56. A.A. Dongargaonkar, and J.D. Clogston, *Humana Press*, New York, NY (2018) 57–63.
57. S. Kim, S.Y. Lee, H.J. Cho, *Nanomaterials* **7**(11), 354 (2017)
58. A. Ivask, I. Kurvet, K. Kasemets, I. Blinova, V. Aruoja, S. Suppi, H. Vija et al., *PLoS ONE* **9**, e102108 (2014)
59. D. Lomelí-Marroquín, D.M. Cruz, A. Nieto-Argüello, A.V. Crua, J. Chen, A. Torres-Castro, T.J. Webster, J.L. Cholula-Díaz, *Int. J. Nanomed.* **14**, 2171–2190 (2019)
60. H.S. Agarwal, V. Kumar, S. Rajeshkumar, *Res. Efficient. Technol.* **3**, 406–413 (2017)
61. M. Murali, C. Mahendra, N. Rajashekar, M.S. Sudarshana, *Spectrochim Acta Part A* **179**, 104–109 (2017)
62. R.C. De Souza, L.U. Haberbeck, H.G. Riella, D.H.B. Ribeiro, B.A.M. Carciofi, *Braz. J. Chem. Eng.* **36**, 885–893 (2019)
63. A. Akbar, M.B. Sadiq, I. Ali, N. Muhammad, Z. Rehman, M.N. Khan, J. Muhammad, S.A. Khan, F.U. Rehman, *Biocatal. Agric. Biotechnol.* **17**, 36–42 (2019)
64. Z.C. Sarillana, E.O. Fundador, N.G. Fundador, *Int. Food Res. J.* **28**(1), 102–109 (2021).
65. S. Shamshad, J. Rashid, I. ul-haq, N. Iqbal, and S. Ullah Awan, *Environ. Eng. Res.* **26**(6), 200454 (2021)
66. K. Dulta, G. Koşarsoy Ağçeli, P. Chauhan et al., *J. Inorg. Organomet. Polym.* **31**, 180–190 (2021)
67. A.A. Menazea, A.M. Ismail, A. Samy, *J. Inorg. Organomet. Polym.* **31**, 4250–4259 (2021)
68. V.B. Raghavendra, S. Shankar, M. Govindappa et al., *J. Inorg. Organomet. Polym.* **32**, 614–630 (2022)
69. J. Jayabalan, G. Mani, N. Krishnan, J. Pernabas, J.M. Devadoss, H.T. Jang, *Biocat. Agr. Biotechnol.* **21**, 101327 (2019)
70. W.M. Abdelraheem, E.S. Mohamed, *J. Infect. Dev. Ctries.* **15**(6), 826–832 (2021)
71. C. Jayaseelan, A.A. Rahuman, A.V. Kirthi, S. Marimuthu, T. Santhoshkumar, A. Bagavan et al., *Spectrochim. Acta A* **90**, 78–84 (2012)
72. P. Rajiv, S. Rajeshwari, R. Venckatesh, *Spectrochim. Acta Part. A* **112**, 384–387 (2013)
73. S. Vijayakumar, B. Vaseeharan, R. Sudhakaran, J. Jeyakandan, P. Ramasamy, A. Sonawane, C. Faggio, *J. Clust. Sci.* **30**, 1465–1479 (2019)
74. D. Jain, A.A. Bhojiya, H. Singh, H.K. Daima, M. Singh, S.R. Mohanty, B.J. Stephen, A. Singh, *Front. Chem.* **8**, 778 (2020)
75. K. Steffy, G. Shanthi, A.S. Maroky, S. Selvakumar, *J. Trace Elem. Med. Biol.* **50**, 229–239 (2018)
76. Y. Hou, Y. Hou, Y. Ren, Y. Shi, X. Jin, Y. Dong, H. Zhang, *Mater Res. Express* **7**, 095015 (2020)
77. S. Mohapatra, L. Leelavathi, M.I. Arumugham et al., *J. Evol. Med. Dent. Sci.* **9**(29), 2034–2039 (2020)
78. M.T.T. Quynh, A.T.N. Hong, D. Van-Dat, T. Quang-Hieu, N. Van Cuong, *J. Nanomater.* **3**, 1–15 (2021)
79. A. Sirelkhatim, S.S. Mahmud, A. Seeni, N.H.M. Kaus, L.C. Ann, S.K.M. Bakhori, H. Hasan, D. Mohamad, *Nano Micro Lett* **7**, 219–242 (2015)
80. R. Pati, R.K. Mehta, S. Mohanty, A. Padhi, M. Sengupta, B. Vaseeharan, C. Goswami, A. Sonawane, *Nanomedicine* **10**, 1195–1208 (2014)
81. A. Akbar, A.K. Anal, *Food Control* **38**, 88–95 (2014)
82. S.X.T. Liang, L.S. Wong, Y.M. Lim, P.F. Lee, S. Djearmane, S. Afr. *J. Chem. Eng.* **34**, 63–71 (2020)
83. S. Soren, S. Kumar, S. Mishra, P.K. Jena, S.K. Verma, P. Parhi, *Microb. Pathog.* **119**, 145–151 (2018)
84. F. Fontecha-Umaña, A.G. Ríos-Castillo, C. Ripolles-Avila, J.J. Rodríguez-Jerez, *Foods* **9**, 442 (2020)
85. P. Swain, S.K. Nayak, A. Sasmal, T. Behera, S.K. Barik, S.K. Swain, S.S. Mishra, A.K. Sen, J.K. Das, P. Jayasankar, *World J. Microbiol. Biotechnol.* **30**(9), 2491–2502 (2014)
86. H. Mohd Yusof, N. Abdul Rahman, R. Mohamad, U. Hasanah Zaidan, A.A. Samsudin, *Animals* **11**, 2093 (2021)
87. N. Talebian, S.M. Amininezhad, M. Doudi, *J. Photochem. Photobiol. B. Biol.* **120**, 66–73 (2013)
88. H. Upadhyaya, S. Shome, R. Sarma et al., *Am. J. Plant Sci.* **9**, 1279–1291 (2018)
89. M. Khatami, H.Q. Alijani, H. Heli, I. Sharifi, *Ceram. Int.* **44**, 15596–15602 (2018)
90. S. Saif, A. Tahir, T. Asim et al., *Saudi J. Biol. Sci.* **26**, 1364–1371 (2019)
91. B.K. Sharma, B.R. Mehta, E.V. Shah, V.P. Chaudhari, D.R. Roy, S.M. Roy, *J. Clust. Sci.* (2021). <https://doi.org/10.1007/s10876-021-02145-x>

92. H. Agarwal, A. Nakara, V.K. Shanmugam, *Biomed. Pharmacother.* **109**, 2561–2572 (2019)
93. N. Jones, B. Ray, R.T. Koodali, A.C. Manna, F.E.M.S. *Microbiol. Lett.* **279**, 71–76 (2008)
94. A. Azam, A.S. Ahmed, M. Oves, M.S. Khan, S.S. Habib, A. Memic, *Int. J. Nanomed.* **7**, 6003–6009 (2012)
95. T. Ohira, O. Yamamoto, *Chem. Engin. Sci.* **68**(1), 355–361 (2012)
96. A.C. Janaki, E. Sailatha, S. Gunasekaran, *Spectrochim Acta Part A* **144**, 17–22 (2015)
97. G.S. Thirumoorthy, O. Balasubramaniam, P. Kumaresan et al., *BioNanoSci.* **11**(1), 172–181 (2021)
98. K. Elumalai, S. Velmurugan, *Appl. Surface Sci.* **345**, 329–336 (2015)
99. S. Rajeshkumar, P. Sivaperumal, M. Tharani, T. Lakshmi, *J. Complement. Med. Res.* **11**(5), 128–136 (2020)
100. B. Sumanth, T.R. Lakshmeesha, M.A. Ansari, M.A. Alzohairy, A.C. Udayashankar, B. Shobha, S.R. Niranjana, C. Srinivas, A. Almatroudi, *Int. J. Nanomed.* **15**, 8519–8536 (2020)
101. K. Velsankar, S. Sudhahar, G. Parvathy et al., *Mater. Chem. Phys.* **239**, 121976 (2020)
102. T. Naseem, T. Durrani, *Environ. Chem. Ecotoxicol.* **3**, 59–75 (2021)
103. (US), National institutes of health, and biological sciences curriculum study, Understanding cancer NIH curriculum supplement series (available at, www.ncbi.nlm.nih.gov/books/NBK20362/) (2007).
104. R.L. Siegel, K.D. Miller, A. Jemal, *Cancer J. Clin.* **69**, 7–34 (2019)
105. A. Pavlopoulou, Y. Oktay, K. Vougas, M. Louka, C.E. Vorgias, A.G. Georgakilas, *Cancer Lett.* **380**, 485–493 (2016)
106. E. Mostafavi, P. Soltantabar, and T.J. Webster, Eds: Y. Lei, B. Sarit, W. Thomas (Elsevier) (2019) 191–212.
107. Y.L. Su, S.H. Hu, *Pharmaceutics* **10**, E193 (2018)
108. J. Jiang, J. Pi, and J. Cai, *Bioinorg. Chem. Appl.* (2018) 1–18.
109. S.A. Akintelu, A.S. Folorunso, *Bionanosci.* **10**, 848–863 (2020)
110. D. Medina Cruz, E. Mostafavi, A. Vernet-Crua, H. Barabadi, V. Shah, J.L. Cholula-Díaz, G. Guisbiers, T.J. Webster, *J. Phys. Mater.* **3**, 4005 (2020)
111. Y. Mostafa, K. Shameli, R. Rasit Ali, S.W. Pang, S.Y. Teow, *J. Mol. Struct.* **1204**, 127–539 (2020)
112. G. Sharma, A. Kumar, S. Sharma, M. Naushad, R. Prakash Dwivedi, Z.A. AlOthman, G.T. Mola, *J. King Saud. Univ. Sci.* **31**, 257–269 (2019)
113. V.P. Shilpa, B. Samuel Thavamani, E.R. Roshni, V.U. Sangeetha, M.S. Panicker, S. Bhagyasree, G. Jilsha, K. Muddukrishnaiah, *Nanomed. Res. J.* **5**(3), 298–305 (2020)
114. A. Aldalbahi, S. Alterary, R.A. Almoghim, M.A. Awad, N.S. Aldosari, S.F. Alghannam et al., *Molecules* **25**, 4198 (2020)
115. P. Bhattacharya, K. Chatterjee, S. Swarnakar, S. Banerjee, *Adv. Nan. Res.* **3**(1), 15–27 (2020)
116. R. Parthasarathy, R. Ramachandran, Y. Kamaraj, S. Dhayanlan, *J. Clust. Sci.* (2021). <https://doi.org/10.1007/s10876-020-01941-1>
117. H.K. Abdelhakim, E.R. El-Sayed, F.B. Rashidi, *J. Appl. Microbiol.* **128**, 1634–1646 (2020)
118. K. Manimaran, G. Balasubramani, C. Ragavendran, D. Natarajan, S. Murugesan, *J. Clust. Sci.* **32**, 1635–1647 (2021)
119. M.M. Housseiny, E.Z. Gomaa, *Egypt. J. Bot.* **59**, 319–337 (2019)
120. Y. Mbenga, M.N. Mthiyane, T.L. Botha et al., *J. Inorg. Organomet. Polym.* (2022). <https://doi.org/10.1007/s10904-022-02248-6>
121. G. Gunalan, K. Vijayalakshmi, A. Saraswathy, W. Hopper, T. Tamilvannan, *J. Chem. Pharm. Res.* **6**, 334–348 (2014)
122. C.S. Williams, M. Mann, R.N. DuBois, *Oncogen* **18**, 7908–7916 (2000)
123. R.A.W. Macrophages, M. Kim, H. Jeong, *Nanosci. Nanotechnol.* **15**, 6509–6515 (2015)
124. H. Agarwal, V.K. Shanmugam, *Bioorg. Chem.* **94**, 103423 (2020)
125. S. Vijayakumar, Z.I. Gonzalez-Sanchez, B. Malaikozhundan, K. Saravanakumar, M. Divya, B. Vaseeharan, E.F. Duran-Lara, M. Wang, *J. Clust. Sci.* **32**, 1129–1139 (2021)
126. M. Ilves, J. Palomaki, M. Vippola et al., *Particle Fibre Toxicol.* **11**(1), 38 (2014)
127. P.C. Nagajyothi, S.J. Cha, I.J. Yang, T.V. Sreekanth, K.J. Kim, H. Shin, *J. Photochem. Photobiol. B* **146**, 10–17 (2015)
128. F. Shao, A.J. Yang, D.M. Yu, J. Wang, X. Gong, H.X. Tian, *J. Photochem. Photobiol. B.* **189**, 267–273 (2018)
129. K.M. Ezealisiji, X. Siwe-Noundou, B. Maduelosi, N. Nwachukwu, R.W.M. Krause, *Int. Nano. Lett.* **9**, 99 (2019)
130. M.M. Mihai, M.B. Dima, B. Dima, A.M. Holban, *Materials (Basel)* **12**, 1–16 (2019)
131. M. Batool, S. Khurshid, Z. Qureshi, W.M. Daoush, *Chem. Pap.* (2020). <https://doi.org/10.1007/s11696-020-01343-7>
132. U.D.S. Sekhon, A. Sen Gupta, A.C.S. Biomaterial, *Sci. Engin.* **4**(4), 1176–1192 (2018)
133. B. Bao, A.S. Prasad, F.W.J. Beck, J.T. Fitzgerald, D. Snell, G.W. Bao, T. Singh, L.J. Cardozo, *Am. J. Clin. Nut.* **91**(6), 1634–1641 (2010)
134. Q. Chen, M. Jin, F. Yang, J. Zhu, Q. Xiao, and L. Zhang, *Med. Inflamm.* (2013) 928315.
135. H. Chen, R. Yada, *Trend Food Sci. Technol.* **22**(11), 585–594 (2011)
136. E.R. Moatamed, A.A. Hussein, M.M. El-Desoky, Z.E. Khayat, *Toxicol. Ind. Health* **35**, 627–637 (2019)
137. T. Zhang, H. Sun, Z. Lv, L. Cui, H. Mao, P.M. Kopittke, *J. Agr. Food Chem.* **66**(11), 2572–2579 (2018)
138. S. Moghaddasi, A. Fotovat, F. Karimzadeh, H.R. Khazaei, R. Khorassani, A. Lakzian, *Arch. Agron. Soil Sci.* **63**(8), 1108–1120 (2017)
139. Rameshraddy, G.J. Pavithra, B.H. Rajashekar Reddy, M. Salimath, K.N. Geetha, A.G. Shankar, *Ind. J. Plant Physiol.* **22**, 287–294 (2017)
140. P.K. Tiwari, M.Sc. Thesis, Anand Agriculture University, India (2017).
141. Z.A. Siddiqui, M.R. Khan, E.F. Abdallah, A. Parveen, *Int. J. Veg. Sci.* (2018) 1–22.
142. R. Bala, A. Kalia, S.S. Dhaliwal, *J. Soil Sci. Plant Nut* **19**, 379–389 (2019)
143. J. Garcia-López, G. Nino-Medina, E. Olivares-Saenz, R. Lira-Saldivar, E. Barriga-Costro, R. Vázquez-Alvarado, P. Rodriguez-Salinas, F. Zavala-Garcia, *Plants* **8**(254), 1–20 (2019)
144. Z. Seydmohammadi, Z. Roein, S. Rezvanipour, *Plant Physiol. Rep.* **74**, 114–119 (2019)
145. R. Shahhoseini, M. Azizi, J. Asili, N. Moshtaghi, L. Samiei, *Acta Physiol. Plant.* **17**, 1–18 (2020)
146. M.S. Sadak, B.A. Bakry, *Bull. Natl. Res. Cent.* **2**, 44–98 (2020)
147. S. Torabian, M. Zahedi, A. Khoshgoftarmansh, *J. Agric. Sci. Technol.* **18**(4), 1013–1025 (2016)
148. H.F. Alharby, E.M.R. Metwali, M.P. Fuller, A.Y. Aldhebani, *Saud. J. Biol. Sci.* **23**, 773–781 (2016)
149. AAH Abdel Latef, MF Abu Alhmad, and KE Abdelfattah, *J. Plant Growth Regul* **36**, 60–70 (2017)
150. L. Vojodi Mehrabani, M.B. Hassan Pouraghdam, T. Shamsi-Khotab, *Acta Sci. Polon Horticulture* **17**(6), 65–73 (2018)
151. M.M. Hussein, N.H. Abou-Baker, *R Soc. Open Sci.* **5**, 171809 (2018)
152. Z. Wang, H. Li, X. Li, C. Xin, J. Si, S. Li, Y. Li, X. Zheng, H. Li, X. Wei, Z. Zhang, L. Kong, F. Wang, *Arch. Agron. Soil Sci.* **66**, 1259–1273 (2020)
153. Z. Noohpisheh, H. Amiri, A. Mohammadi, S. Farhadi, *Int. J. Deal. Aspect Plant. Biol.* **155**(2), 267–280 (2020)

154. N. Taran, V. Storozhenko, N. Sviatlova, L. Batsmanova, V. Shvartau, M. Kovalenko, *Nanoscale Res. Lett.* **12**, 60 (2017)
155. C.O. Dimkpa, U. Singh, P.S. Bindraban, W.H. Elmer, J.L. Gardea-Torresdey, J.C. White, *Sci. Total. Environ.* **688**, 926–934 (2019)
156. A.M. Dhalimi, S.A.H. Ajeel, *Plant Arch.* **20**, 2720–2725 (2020)
157. L. Sun, F. Song, X. Zhu, S. Liu, F. Liu, Y. Wang, Z. Li, *Arch. Agron. Soil Sci.* **67**(2), 245–259 (2020)
158. R. Kumar, A. Umar, G. Kumar, H.S. Nalwa, *Ceram. Int.* **43**, 3940–3961 (2017)
159. M. Saghian, S. Dehghanpour, M. Sharbatdaran, *RSC Adv.* **10**, 9369–9377 (2020)
160. K.G. Akpomie, J. Conradie, *Sci. Rep.* **10**, 17094 (2020)
161. M. Alkasir, N. Samadi, Z. Sabouri, Z. Mardani, M. Khatami, M. Darroudi, *Inorg. Chem. Commun.* **119**, 108066 (2020)
162. S.P. Rajendran, K. Sengodan, *J. Nanosci.* (2017). <https://doi.org/10.1155/2017/8348507>
163. R. Vinayagam, R. Selvaraj, P. Arivalagan, T. Varadavenkatesan, *J. Photochem. Photobiol. B* **203**, 111760 (2020)
164. S.S. Shabnam, S.S. Meenu, K.A. Yadavendra, *Adv. Biotech. Micro.* **2**(3), 74–80 (2017)
165. B. Divya, C. Karthikeyan, M. Rajasimman, *Int. J. Nanosci. Nanotechnol.* **14**(4), 267–275 (2018)
166. V. Goyal, A. Singh, J. Singh, T. Singh, A.A. Al-Kheraif, H. Kaur, S. Kumar, M. Rawat, *J. Clust. Sci.* (2021). <https://doi.org/10.1007/s10876-021-02108-2>
167. T. Bhuyan, K. Mishra, M. Khanuja, R. Prasad, A. Varma, *Mater. Sci. Semicond. Process* **32**, 55–61 (2015)
168. O.J. Nava, C.A. Soto-Robles, C.M. Gómez-Gutiérrez, A.R. Vilchis-Nestor, A. Castro-Beltrán, A. Olivás et al., *J. Mol. Struct.* **1147**, 1–6 (2017)
169. A. Spoială, C.I. Ilie, R.D. Truscă, O.C. Oprea, V.A. Surdu, B.S. Vasile, A. Fica, D. Fica, E. Andronescu, L.M. Ditu, *Materials* **14**, 4747 (2021)
170. T. Karnan, S.A.S. Selvakumar, *J. Mol. Struct.* **1125**, 358–365 (2016)
171. A.A. Ali, I.S. Ahmed, A.S. Amin et al., *J. Inorg. Organomet. Polym.* **31**, 3780–3792 (2021)
172. M.J. Osmond, M.J. McCall, *Nanotoxicology* **4**, 15–41 (2010)
173. R.K. Ibrahim, M. Hayyan, M.A. AlSaadi, A. Hayyan, S. Ibrahim, *Environ. Sci. Pollut. Res.* **23**, 13754–13788 (2016)
174. L. Pagano, F. Pasquali, S. Majumdar, R.D. Torre-Roche, N. Zuverza-Mena, M. Villani, A. Zappettini, R.E. Marra, S.M. Isch et al., *Environ. Sci. Nano* **4**, 1579–1590 (2017)
175. E. Yusefi-Tanha, S. Fallah, A. Rostamnejadi, L.R. Pokhrel, *Sci. Total. Environ.* **10**(738), 140240 (2020)
176. N. Zuverza-Mena, D. Martínez-Fernández, W. Du, J.A. Hernandez-Viezcas, N. Bonilla-Bird et al., *Plant Physiol. Biochem.* **110**, 236–264 (2017)
177. I. Pujalte, I. Passagne, B. Brouillaud, M. Treguer, E. Durand, C. Ohayon-Courtes et al., *Part Fibre Toxicol.* **8**(1), 1–16 (2011)
178. H. Najafzadeh, S.M. Ghoreishi, B. Mohammadian, E. Rahimi, M.R. Afzalzadeh, M. Kazemivarnamkhasti et al., *Vet. World* **6**(8), 10 (2013)
179. S. Saman, S. Moradhaseli, A. Shokouhian, M. Ghorbani, *Adv. Biores.* **4**(2), 83–88 (2013)
180. C. Wang, J. Lu, L. Zhou, J. Li, J. Xu, W. Li et al., *PLoS ONE* **11**, e0164434 (2016)
181. R. Kumar, I. Roy, T.Y. Ohulchanskyy, L.A. Vathy, E.J. Bergey, M. Sajjad et al., *ACS Nano* **4**, 699–708 (2010)
182. R. Wahab, N. Kaushik, F. Khan, N.K. Kaushik, E.H. Choi, J. Musarrat et al., *Sci. Rep.* **6**, 19950 (2016)
183. S. Singh, *Toxicol. Mech. Method* **29**(4), 300–311 (2019)
184. P.K. Babel, P.K. Thakre, R. Kumawat, R.S. Tomar, *Chemosphere* **213**, 65–75 (2018)
185. S. Busi, J. Rajkumari, S. Pattnaik, P. Parasuraman, S. Hnamte, *J. Microbiol. Biotechnol. Food Sci.* **05**, 407–411 (2016)
186. M. Taran, M. Rad, and M. Alavi, *BioImpacts* **8** (2018).
187. K. Prasad, A.K. Jha, *Nat. Sci.* **01**, 129–135 (2009)
188. B.N. Singh, A.K.S. Rawat, W. Khan, A.H. Naqvi, B.R. Singh, *PLoS ONE* **9**, e106937 (2014)
189. D. Kundu, C. Hazra, A. Chatterjee, A. Chaudhari, S. Mishra, *J. Photochem. Photobiol. B* **140**, 194–204 (2014)
190. N. Rajabairavi, C.S. Raju, C. Karthikeyan, K. Varutharaju, S. Nethaji, A.S.H. Hameed et al., *Springer Proc. Phys.* **189**, 245–254 (2017)
191. B. Balraj, N. Senthilkumar, C. Siva, R. Krithikadevi, A. Julie, I.V. Potheher et al., *Res. Chem. Intermed.* **43**, 2367–2376 (2017)
192. M.A. Shamsuzzaman, H. Khanam, R.N. Aljawfi, *Arab. J. Chem.* **10**, 1530–1566 (2017)
193. J. Sarkar, M. Ghosh, A. Mukherjee, D. Chattopadhyay, K. Acharya, *Bioprocess. Biosyst. Eng.* **37**, 165–171 (2014)
194. A. Rajan, E. Cherian, G. Baskar, *Int. J. Mod. Sci. Technol.* **1**, 52–57 (2016)
195. G. Baskar, J. Chandhuru, K.S. Fahad, A.S. Praveen, *Asian J. Pharm. Technol.* **3**, 142–146 (2013)
196. P. Velmurugan, J. Shim, Y. You, S. Choi, S. Kamala-Kannan, K.J. Lee et al., *J. Hazard Mater* **182**, 317–324 (2010)
197. Y. Jiang, L. Zhang, D. Wen, Y. Ding, *Mater. Sci. Eng. C* **69**, 1361–1366 (2016)
198. K. Ghule, A.V. Ghule, B.J. Chen, Y.C. Ling, *Green Chem.* **8**(12), 1034–1041 (2006)
199. K.M. Reddy, K.F. Feris, J. Bell, D.G. Wingett, C. Hanley, A. Punnoose, *Appl. Phys. Lett.* **90**, 21 (2007)
200. S. Sarwar, S. Chakraborti, S. Bera, I.A. Sheikh, K.M. Hoque, P. Chakrabarti, *Nanomed. Nanotechnol. Biol. Med.* **12**(6), 1499–1509 (2016)
201. W. Salem, D.R. Leitner, F.G. Zingl et al., *Int. J. Med. Microbiol.* **305**(1), 85–95 (2015)
202. I. Matai, A. Sachdev, P. Dubey, S.U. Kumar, B. Bhushan, P. Gopinath, *Colloids Surf. B* **115**, 359–367 (2014)
203. M. Shaban, F. Mohamed, S. Abdallah, *Sci. Rep.* **8**(1), 3925 (2018)
204. X. Bellanger, P. Billard, R. Schneider, L. Balan, C. Merlin, *J. Hazard. Mater.* **283**, 110–116 (2015)
205. K. Karthik, S. Dhanuskodi, C. Gobinath, S. Sivaramkrishnan, *Spectrochim. Acta Part A* **139**, 7–12 (2015)
206. M. Ramani, S. Ponnusamy, C. Muthamizhchelvan, J. Cullen, S. Krishnamurthy, E. Marsili, *Colloids Surf. B* **105**, 24–30 (2013)
207. I. De Angelis, F. Barone, A. Zijno et al., *Nanotoxicology* **7**(8), 1361–1372 (2013)
208. Y. Cao, M. Roursgaard, A. Kermanizadeh, S. Loft, P. Moller, *Int. J. Toxicol.* **34**(1), 67–76 (2015)
209. V. Sharma, D. Anderson, A. Dhawan, *Apoptosis* **17**(8), 852–870 (2012)
210. M.J. Akhtar, M. Ahamed, S. Kumar, M.M. Khan, J. Ahmad, S.A. Alrokayan, *Int. J. Nanomed.* **7**, 845–857 (2012)
211. S. Majeed, M. Danish, F.S.B. Norazmi, *Adv. Sci. Eng. Med.* **10**, 551–556 (2018)
212. N. Tripathy, R. Ahmad, H.A. Ko, G. Khang, Y.B. Hahn, *Nanoscale* **7**(9), 4088–4096 (2015)
213. G. Baskar, J. Chandhuru, K. Sheraz Fahad, A.S. Praveen, M. Chamundeeswari, T. Muthukumar, *J. Mater. Sci. Mater. Med.* **26**, 43 (2015)
214. J. Liu, X. Ma, S. Jin et al., *Mol. Pharm.* **13**(5), 1723–1730 (2016)
215. X. Fang, L. Jiang, Y. Gong, J. Li, L. Liu, Y. Cao, *Chem. Biol. Int.* **278**, 40–47 (2017)
216. B.A. Othman, C. Greenwood, A.F. Abuelela, *Adv. Healthcare Mat.* **5**(11), 1310–1325 (2016)

Publisher's Note Springer Nature remains neutral with regard to jurisdictional claims in published maps and institutional affiliations.